

UC Davis

UC Davis Previously Published Works

Title

Vaping Aerosols from Vitamin E Acetate and Tetrahydrocannabinol Oil: Chemistry and Composition

Permalink

<https://escholarship.org/uc/item/95p647n1>

Journal

Chemical Research in Toxicology, 35(6)

ISSN

0893-228X

Authors

Li, Yichen

Dai, Jiayin

Tran, Lillian N

et al.

Publication Date

2022-06-20

DOI

10.1021/acs.chemrestox.2c00064

Peer reviewed

# Vaping Aerosols from Vitamin E Acetate and Tetrahydrocannabinol Oil: Chemistry and Composition

Yichen Li, Jiayin Dai, Lillian N. Tran, Kent E. Pinkerton, Eliot R. Spindel, and Tran B. Nguyen\*



Cite This: <https://doi.org/10.1021/acs.chemrestox.2c00064>



Read Online

ACCESS |



Metrics & More

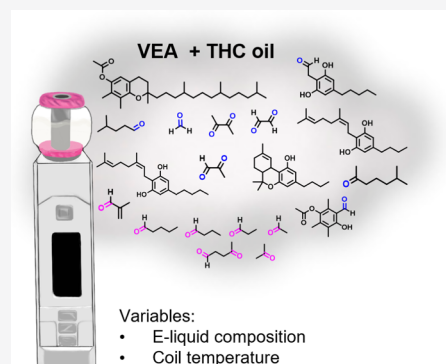


Article Recommendations



Supporting Information

**ABSTRACT:** The popularity of vaping cannabis products has increased sharply in recent years. In 2019, a sudden onset of electronic cigarette/vaping-associated lung injury (EVALI) was reported, leading to thousands of cases of lung illness and dozens of deaths due to the vaping of tetrahydrocannabinol (THC)-containing e-liquids that were obtained on the black market. A potential cause of EVALI has been hypothesized due to the illicit use of vitamin E acetate (VEA) in cannabis vape cartridges. However, the chemistry that modifies VEA and THC oil, to potentially produce toxic byproducts, is not well understood under different scenarios of use. In this work, we quantified carbonyls, organic acids, cannabinoids, and terpenes in the vaping aerosol of pure VEA, purified THC oil, and an equal volume mixture of VEA and THC oil at various coil temperatures (100–300 °C). It was found under the conditions of our study that degradation of VEA and cannabinoids, including  $\Delta^9$ -THC and cannabigerol (CBG), occurred via radical oxidation and direct thermal decomposition pathways. Evidence of terpene degradation was also observed. The bond cleavage of aliphatic side chains in both VEA and cannabinoids formed a variety of smaller carbonyls. Oxidation at the ring positions of cannabinoids formed various functionalized products. We show that THC oil has a stronger tendency to aerosolize and degrade compared to VEA at a given temperature. The addition of VEA to the e-liquid nonlinearly suppressed the formation of vape aerosol compared to THC oil. At the same time, toxic carbonyls including formaldehyde, 4-methylpentanal, glyoxal, or diacetyl and its isomers were highly enhanced in VEA e-liquid when normalized to particle mass.



## 1. INTRODUCTION

The unexpected outbreak of e-cigarette or vaping-associated lung injury (EVALI) was reported nationwide beginning in September 2019, causing more than 2800 hospitalizations and 60 deaths.<sup>1–4</sup> The specific biological mechanisms of EVALI, as well as the chemical causes, are still under investigation.<sup>5–8</sup> Evidence shows that EVALI is associated with vaping tetrahydrocannabinol (THC) containing e-liquid cartridges that were obtained on the black market.<sup>9–12</sup> Although adverse health effects of vaping THC cartridges have been found to include abdominal pain, nausea, chest pain, shortness of breath, and acute respiratory distress,<sup>13–15</sup> they have not to date been fatal. In contrast, sudden deaths and hospitalizations from EVALI were linked to a compound called vitamin E acetate (VEA), the chemically stable esterified form of vitamin E (VE).<sup>3,16–18</sup> VEA is thought to have been used as a cutting or diluting agent in THC cartridges because it has a similar viscosity to THC oil,<sup>16</sup> therefore allowing the dilution or adulteration of the THC oil as a means to increase profit margins while not being visually evident.<sup>19</sup> FDA laboratories confirmed that VEA was present in 81% of THC-containing vaping cartridges confiscated from 93 EVALI patients.<sup>20</sup> VEA was also found in the bronchoalveolar (BAL) fluid samples from 48 of 51 patients but not in samples from the healthy comparison control group.<sup>21–23</sup> The VEA fraction in vaping cartridges confiscated

from EVALI patients ranged from 23 to 88%.<sup>18,24</sup> Duffy et al.<sup>18</sup> analyzed 38 samples of 10 EVALI cases in New York and found a VEA content of up to ~58% and a  $\Delta^9$ -THC content of up to ~66% in the confiscated cartridges. This work aims to study vaping aerosols from e-liquids relevant to the content of these cartridges in a controlled laboratory setting.

Both aerosolized VEA itself<sup>25,26</sup> and its thermal degradation products<sup>27,28</sup> were shown to be toxic or potentially toxic in vivo. However, currently, there is not sufficient evidence to rule out the contribution of other ingredients in the confiscated cannabis vaping e-liquids<sup>29,30</sup> (such as cannabinoids, terpenoids, pesticides used in the cultivation of marijuana, alkanes used for extraction, etc.) or their synergistic effects<sup>16,24</sup> with VEA. Terpenes in cannabis vapes,<sup>31</sup> for example, can also degrade into toxic products such as benzene and methacrolein.<sup>30,32</sup> Radiological and histological analyses of some EVALI patients did not find exclusive evidence of lipoid pneumonia that would be

Received: February 23, 2022

expected from the lipid-like VEA in some cases of lung injury.<sup>33,34</sup> Instead, ground glass opacities and other observations have been made that could implicate smaller toxic compounds, instead of (or in addition to) inhaled VEA. *In vitro* and animal studies also suggest that pure VEA is not entirely equivalent to confiscated vape cartridges in its biological effects.<sup>35</sup> Thus, it is important to study the mixture of VEA with cannabis-based extracts to understand whether VEA has unique, additive, or synergistic effects modifying the chemical characteristics or biological effects of the aerosol that is vaped.

It is also not clear if extreme temperatures and/or use conditions are required for toxicant formation that contribute to EVALI. Temperatures that are sufficiently high to initiate combustion and pyrolysis may produce, for example, toxic ketene gas from VEA.<sup>28</sup> Although high temperatures may occur under certain conditions of use, including those potentially associated with EVALI,<sup>36,37</sup> users may also choose to avoid such scenarios due to unpleasant sensations and taste.<sup>38,39</sup> This study focuses on a detailed characterization of the composition and degradation chemistry of vaping aerosols from VEA, purified THC oil, and a mixture of the two, in a temperature-programmable third-generation “mod” device and using puffing regimen that is consistent with CORESTA recommendations.<sup>40</sup> A temperature range of 100–300 °C was chosen to represent wet- or partially wet wick conditions for mods and clearomizers,<sup>38,41,42</sup> which is sufficient to degrade VEA.<sup>27,43</sup> Gravimetric analysis is used to evaluate aerosolization efficiency. High-performance liquid chromatography coupled with high-resolution mass spectrometry (HPLC-HRMS)<sup>44</sup> is used to characterize thermal degradation carbonyls and acids, as well as cannabinoids and oxidized cannabinoids. Gas chromatography–mass spectrometry (GC-MS) was used to quantify particle-phase terpenoids. Thermal degradation and mechanisms for the oxidation of THC and VEA are proposed, which may prove useful for policy guidance and future research.

## 2. EXPERIMENTAL SECTION

**2.1. Vaping Aerosol Generation and Collection.** A temperature-controlled third-generation Evolv DNA 75 modular e-cigarette device (Evolv LLC, Hudson, OH) with a refillable e-liquid tank and single-mesh stainless steel coils (SS316L, FreeMax, Inc., Shenzhen, China) was used for aerosol generation (hereinafter referred to as the “mod”, Figure 1). The mod enabled variable output voltages (0.2–9 V) with a coil resistance of ~0.12 Ω. This device allows for temperature control and facile coil temperature measurements. Evolv Escribe software (Evolv LLC, Hudson, OH) was used to customize the power output (0–75 W) to achieve the desired coil temperature. Coil temperature was measured by a flexible Kapton-insulated K-type thermocouple (Oakton Instruments, Inc., Vernon Hills, IL) in contact with the center of the coil surface and output to a digital readout. The temperature set by the device is not truly representative of the measured coil temperature.<sup>45</sup> Discrepancies between set and measured coil temperature arise from variations in the air flow rate, e-liquid viscosity, and coil resistance (from material/batch), which alter the relationship between applied power and output temperature that drive aerosol chemistry. The puff duration is 3 s with a flow rate of 1.1–1.2 L/min, quantified by a primary flow calibrator (A.P. Buck, Inc., Orlando, FL), corresponding to a puff volume of 55–60 mL.<sup>46</sup> The e-liquids used for vaping in this work are: (1) pure VEA (purity ≥ 96%, Sigma-Aldrich, St. Louis, MO), (2) purified THC oil extracted from cannabis (NatuEra, ESP-071, subsequently referred to as “THC oil” for brevity); and (3) a mixture of VEA and THC oil (volume ratio of 1:1). The THC oil was commercially obtained from Biopharmaceutical Research Company (BRC, Castroville, CA), and all work was performed in the BRC facility under their DEA licensure. Composition analysis of the cannabinoid content of the THC oil (Figure S1) demonstrated the most abundant

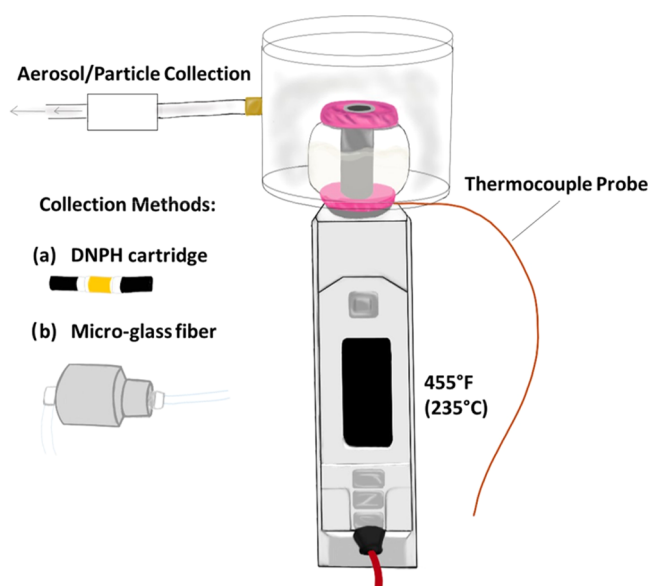


**Figure 1.** Setup of vaping device (mod) and collection system. The particulate fraction of vaping aerosol will be collected glass fiber filter. Carbonyls, acids, and cannabinoids in aerosol will be collected on a 2,4-DNP cartridge for the HPLC-HRMS analysis.

cannabinoids to be:  $\Delta^9$ -tetrahydrocannabinol (THC, mass percentage ~33%),  $\Delta^9$ -tetrahydrocannabinol acid (THCA, ~33%), and cannabigerolic acid (CBGA, mass percentage of 11%). The certificate of analysis of the THC oil advertises 40–60% dry weight of  $\Delta^9$ -THC, with <5% of CBD and CBN; thus, the THCA and CBDA contents may not have been included in the original analysis or may have been converted from their neutral counterparts prior to receipt of the materials. Duffy et al.<sup>18</sup> also found THCA in confiscated cannabis vapes associated with EVALI. All other cannabinoids were found to be below 3% of the total peak area (e.g., cannabidiol, cannabigerol, tetrahydrocannabivarin, cannabichromene, etc.).  $\Delta^8$ -THC, with a retention time of 0.3 min after the  $\Delta^9$  isomer, was not detected in the mixture. THC oil presumably also contains terpenoids, alkanes, and alkenes, although these were not able to be characterized in the unvaped e-liquid. Three temperatures (315, 450, 545 °F (corresponding to 157, 232, 285 °C) were chosen for the particle generation within the range of the vaping device, with a temperature variance of 10–20 °F.

Carbonyls, acids, and cannabinoids in the vaping aerosol (both gas and particles), which represent the majority of expected products,<sup>27,29</sup> were collected onto 2,4-dinitrophenylhydrazine (2,4-DNP) cartridges (Supelco, Inc., 350 mg DNP, Bellefonte, PA) for HPLC-HRMS analysis. A total of 10 puffs of aerosol with a frequency of 2 puffs/min was loaded onto the cartridge. Consecutive sampling with three DNP cartridges demonstrated a collection efficiency >98.4% for carbonyl-DNP adducts in the first cartridge.<sup>47</sup> DNP was conserved in the cartridge after the collection to maximize derivatization efficiency (Figure S2). DNP cartridges were extracted with 2 mL of acetonitrile (Fisher Scientific, Inc., LC-MS grade, Hapton, NH) into autosampler vials and analyzed by HPLC-HRMS. Consecutive extractions of DNP cartridges for samples confirmed that >97% of both DNP and its hydrazones were extracted after the first 2 mL volume of acetonitrile. Cannabinoids were trapped in the silica without modification. The collection efficiency for cannabinoids is unknown, as only a limited amount of THC oil was available for experimentation, thus quality control tests were not performed. Glass fiber filters (Pall Corp., New York) were used to collect the aerosolized particulates as in other e-cigarette studies.<sup>46</sup> Glass fiber filter and DNP cartridge collection of aerosols occurred separately. The particulate mass collected on filters was determined gravimetrically on a microbalance (Mettler Toledo, Inc., 0.0001 g readability, calibrated by weight standards) by weighing the filter mass immediately before and after puffing under the specified experimental conditions. Particles on polytetrafluoroethylene (PTFE)

filters were also collected for select chemical analyses. Due to potential losses of particles through the collection apparatus, particle measurements are used in this work to indicate relative changes due to e-liquid composition or coil temperature instead of absolute quantities. The standard deviation of triplicate gravimetric analysis was determined to be ~20%, primarily due to variations in puffing idiosyncrasies of the mod. Chemical analyses were also performed in triplicate, and standard deviation of the data are reported in relation to the specific analysis performed.

**2.2. Chemical Characterization of Carbonyls, Acids, and Cannabinoids by High-Performance Liquid Chromatography High-Resolution Mass Spectrometry (HPLC-HRMS).** Carbonyl compounds and acids derivatized by 2,4-DNPH to hydrazones were analyzed by negative-ion mode electrospray ionization (ESI) using HPLC-HRMS. Details for the quantification and identification of each carbonyl and acid were described by our laboratory previously.<sup>44</sup> Cannabinoids were observed in both the positive- and negative-mode ESI without modification.<sup>48</sup> Concentration calibration of cannabinoids was performed using certified reference materials in methanol (Sigma-Aldrich, Inc.). External mass calibration and concentration calibration of hydrazones were performed using DNPH standard mixtures (M-1004-10X, Accustandard, Inc.) immediately prior to analysis by mass spectrometry. The calibrated mass accuracy was within 1.5 ppm for standard compounds. All molecular assignments were analyzed by the MIDAS v.3.21 molecular formula calculator (Florida State Univ.). Analytes were separated using an Agilent 1100 HPLC with a Poroshell EC-C18 column (2.1 mm × 100 mm, 2.7 μm, 120 Å, Agilent, Inc.) and analyzed with a linear-trap-quadrupole Orbitrap (LTQ-Orbitrap) mass spectrometer (Thermo Corp., Waltham, MA) with a mass resolving power of ~60 000  $m/\Delta m$  at  $m/z$  400. The mobile phase consisted of LC-MS-grade water with 0.1% formic acid (A) and acetonitrile (B). Elution of analytes occurred over the course of 45 min at 0.27 mL/min with the following gradient program: 40% B (3 min), 50% B (14.3 min), 60% B (20 min), 80% B (40 min), and 40% B (42 min). After separation by chromatography, single-ion chromatography (SIC) of each compound was extracted for the quantification of specific carbonyl compounds based on their calibrated  $m/z$ . Select structural isomers were not separable by this method, so the concentration of these isomers is reported as the total amount. The concentrations of carbonyls for which analytical standards were not available were calculated as described by Li et al.<sup>44</sup>

**2.3. Chemical Characterizations of Terpenoids by Gas Chromatography–Mass Spectrometry (GC-MS).** Particles collected on PTFE filters were extracted using 0.5 mL of ethyl acetate with brief sonication and analyzed with gas chromatography–mass spectrometry (GC-MS) on an Agilent 6890 GC and 5973 MS detector using an HP-5MS column (20 m × 250 μm × 0.25 μm), 2 μL injection at 300 °C (50:1 pulsed split), and the following temperature program: 45 °C (2 min hold), 10 °C min<sup>-1</sup> until 140 °C (0.5 min hold), 30 °C min<sup>-1</sup> until 300 °C (2 min hold). Ethyl acetate is a suitable solvent for extraction and GC analyses of terpenes.<sup>49,50</sup> Calibration was performed using cannabis terpene mixture reference standards in methanol (Sigma-Aldrich, Inc.). The method utilized selected ion monitoring (SIM) acquisition mode with SIM transitions reported elsewhere.<sup>49</sup>

### 3. RESULTS AND DISCUSSION

**3.1. Aerosol Mass and Composition.** Table 1 shows the aerosol particulate mass collected on filters at three temperatures and various e-liquid compositions. Due to the high molecular weight of the e-liquid ingredients, we expect particle mass to be the major fraction of total aerosolized mass. Increasing temperature increased the particle mass collected on the filter, which was consistent with expectations.<sup>51,52</sup> The particle mass production at any particular temperature was suppressed after adding VEA, with pure VEA having the lowest aerosolization efficiency. The aerosolization of e-liquids in response to a heated coil is some combination of thermally induced phase change and chemistry. The thermal stability of THC (<80 °C) is lower

**Table 1. Particle Mass Collected on a Quartz Fiber Filter by Vaping VEA, VEA/Extracted THC Oil, and Extracted THC Oil<sup>a</sup>**

	THC (mg/puff)	THC/VEA (mg/puff)	VEA (mg/puff)
low temperature	1.2 ± 0.2	N.D.	N.D.
medium temperature	10.8 ± 1	1.5 ± 0.2	0.8 ± 0.1
high temperature		5 ± 1	2.7 ± 0.3

<sup>a</sup>Low-temperature range is 315 ± 15 °F (157 °C), medium-temperature range is 450 ± 20 °F (232 °C), and high-temperature range is 545 ± 10 °F (285 °C). N.D. = not detected. The high-temperature data for THC are unavailable.

— Compound identified from vaping aerosol of both pure VEA and extracted THC oil  
 — Compound identified from vaping aerosol of extracted THC oil  
 — Compound identified from vaping aerosol of pure VEA

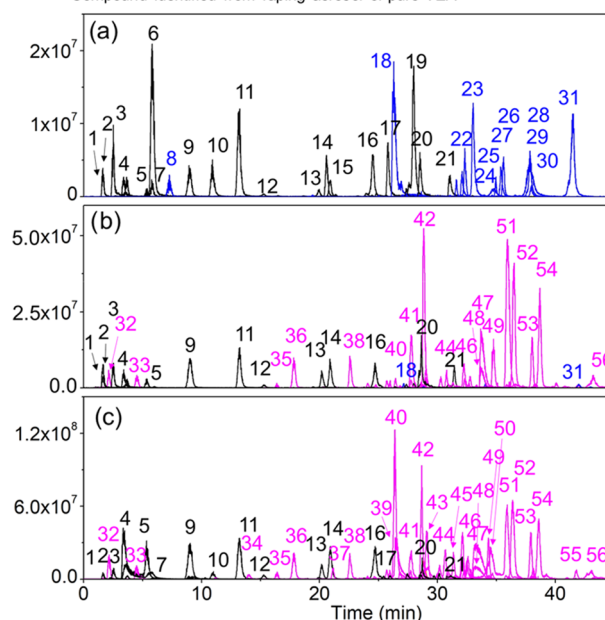


**Figure 2.** Single-ion chromatograms (SIC) of the thermal degradation products and aerosolized components from the vaping aerosol of (a) VEA, (b) 1:1 VEA/THC oil, and (c) THC oil at 450 ± 20 °F (232 °C). Proposed assignments for numbered compounds are shown in Table 2.

compared to VEA (<240 °C); this is similar to the trend of the vacuum boiling points (THC ~ 156 °C at 0.05 mmHg) vs VEA (~220 °C at 0.04 mmHg).<sup>53–55</sup> The normal boiling point of VEA cannot be measured as it degrades before it boils at atmospheric pressure.<sup>53</sup> These thermodynamic properties indicate that it takes more energy to induce a change in VEA compared to THC, whether that change is a change in phase or chemical bonding, consistent with their aerosolization trends and the observation of degradation products during vaping. It is noteworthy that the suppression in aerosol formation did not scale with VEA volume content in the e-liquid at the same temperature, e.g., the 1:1 THC/VEA sample produced only a tenth of the particle mass of the THC sample. It is likely the addition of VEA produces a nonideal solution with the THC oil by introducing significant intermolecular interactions between VEA and cannabinoids. This is consistent with the observation of Lanzarotta et al.<sup>24</sup> that hydrogen bonding occurs between VEA and THC. The number of hydrogen-bond interactions in a mixture is shown to be directly proportional to its viscosity.<sup>56</sup> While the viscosities of the e-liquid solutions tested are not

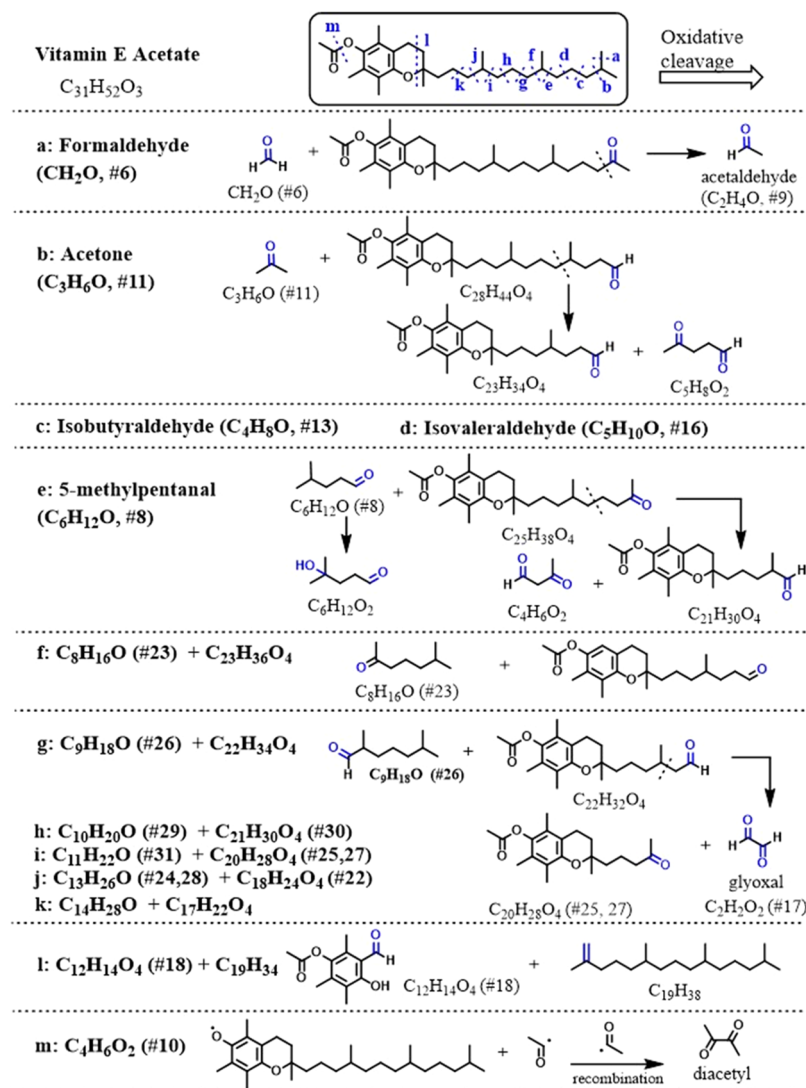
**Table 2. Identification Table for the Cannabinoids and Proposed Thermal Degradation Products Present in Aerosols Sampled from Vaped VEA and THC Oil at 450 ± 20 °F (232 °C)**

peak labeled in chromatograph	calibrated <i>m/z</i>	corresponding ion	mass error (ppm)	molecular formula	proposed compound
Compound Present in Vaping Aerosol of Both Pure VEA and THC Oil					
6	209.032	C <sub>7</sub> H <sub>5</sub> N <sub>4</sub> O <sub>4</sub> <sup>-</sup>	-0.1	CH <sub>2</sub> O	formaldehyde
9	223.047	C <sub>8</sub> H <sub>7</sub> N <sub>4</sub> O <sub>4</sub> <sup>-</sup>	0.1	C <sub>2</sub> H <sub>4</sub> O	acetaldehyde
1	225.027	C <sub>7</sub> H <sub>5</sub> N <sub>4</sub> O <sub>5</sub> <sup>-</sup>	0.3	CH <sub>2</sub> O	formic acid
11	237.063	C <sub>9</sub> H <sub>9</sub> N <sub>4</sub> O <sub>4</sub> <sup>-</sup>	0.3	C <sub>3</sub> H <sub>6</sub> O	acetone
12	237.063	C <sub>9</sub> H <sub>9</sub> N <sub>4</sub> O <sub>4</sub> <sup>-</sup>	0.3	C <sub>3</sub> H <sub>6</sub> O	propionaldehyde
2	239.042	C <sub>8</sub> H <sub>7</sub> N <sub>4</sub> O <sub>5</sub> <sup>-</sup>	0.4	C <sub>2</sub> H <sub>4</sub> O <sub>2</sub>	acetic acid
3	239.042	C <sub>8</sub> H <sub>7</sub> N <sub>4</sub> O <sub>5</sub> <sup>-</sup>	0.4	C <sub>2</sub> H <sub>4</sub> O <sub>2</sub>	glycolaldehyde
14	249.063	C <sub>10</sub> H <sub>9</sub> N <sub>4</sub> O <sub>4</sub> <sup>-</sup>	-0.5	C <sub>4</sub> H <sub>6</sub> O	methacrolein
7	251.042	C <sub>9</sub> H <sub>7</sub> N <sub>4</sub> O <sub>5</sub> <sup>-</sup>	-0.4	C <sub>3</sub> H <sub>4</sub> O <sub>2</sub>	methylglyoxal
13	251.078	C <sub>10</sub> H <sub>11</sub> N <sub>4</sub> O <sub>4</sub> <sup>-</sup>	-0.3	C <sub>4</sub> H <sub>8</sub> O	butyraldehyde or isobutyraldehyde
15	251.078	C <sub>10</sub> H <sub>11</sub> N <sub>4</sub> O <sub>4</sub> <sup>-</sup>	-0.3	C <sub>4</sub> H <sub>8</sub> O	2-butan
4	253.058	C <sub>9</sub> H <sub>9</sub> N <sub>4</sub> O <sub>5</sub> <sup>-</sup>	1.0	C <sub>3</sub> H <sub>6</sub> O <sub>2</sub>	hydroxyacetone,
5	253.058	C <sub>9</sub> H <sub>9</sub> N <sub>4</sub> O <sub>5</sub> <sup>-</sup>	1.0	C <sub>3</sub> H <sub>6</sub> O <sub>2</sub>	lactaldehyde or 1-hydroxypropanal
10	265.058	C <sub>10</sub> H <sub>9</sub> N <sub>4</sub> O <sub>5</sub> <sup>-</sup>	-0.2	C <sub>4</sub> H <sub>6</sub> O <sub>2</sub>	diacetyl or 3-oxopentanal
21	445.086	C <sub>16</sub> H <sub>13</sub> N <sub>8</sub> O <sub>8</sub> <sup>-</sup>	0	C <sub>4</sub> H <sub>6</sub> O <sub>2</sub>	diacetyl or 3-oxobutanol
16	265.094	C <sub>11</sub> H <sub>13</sub> N <sub>4</sub> O <sub>4</sub> <sup>-</sup>	-0.5	C <sub>5</sub> H <sub>10</sub> O	valeraldehyde or isovaleraldehyde
19	279.110	C <sub>12</sub> H <sub>15</sub> N <sub>4</sub> O <sub>4</sub> <sup>-</sup>	0.1	C <sub>6</sub> H <sub>12</sub> O	hexanal or 4-methylpentanal
17	417.054	C <sub>14</sub> H <sub>9</sub> N <sub>8</sub> O <sub>8</sub> <sup>-</sup>	0.2	C <sub>2</sub> H <sub>2</sub> O <sub>2</sub>	glyoxal
20	431.070	C <sub>15</sub> H <sub>11</sub> N <sub>8</sub> O <sub>8</sub> <sup>-</sup>	-0.3	C <sub>3</sub> H <sub>4</sub> O <sub>2</sub>	methylglyoxal
Compound Present in e-Liquid and Vaping Aerosol of THC Oil					
	309.185	C <sub>21</sub> H <sub>25</sub> O <sub>2</sub> <sup>-</sup>	0	C <sub>21</sub> H <sub>26</sub> O <sub>2</sub>	cannabinol (CBN)
48	313.218	C <sub>21</sub> H <sub>29</sub> O <sub>2</sub> <sup>-</sup>	0.3	C <sub>21</sub> H <sub>30</sub> O <sub>2</sub>	tetrahydrocannabinol (THC)
					cannabidiol (CBD)
					cannabichromene (CBC)
42,47	359.222	C <sub>22</sub> H <sub>31</sub> O <sub>4</sub> <sup>-</sup>	0.6	C <sub>21</sub> H <sub>30</sub> O <sub>2</sub> <sup>4a</sup>	tetrahydrocannabinol (THC)
				C <sub>22</sub> H <sub>32</sub> O <sub>4</sub>	cannabigerolic acid (CBGA)
52,53	357.206	C <sub>22</sub> H <sub>29</sub> O <sub>4</sub> <sup>-</sup>	-0.9	C <sub>22</sub> H <sub>30</sub> O <sub>4</sub>	tetrahydrocannabinolic acid (THCA)
	315.233	C <sub>21</sub> H <sub>31</sub> O <sub>2</sub> <sup>-</sup>	0.5	C <sub>21</sub> H <sub>32</sub> O <sub>2</sub>	cannabigerol (CBG)
Compound Present Only in the Vaping Aerosol of THC Oil					
32	269.053	C <sub>9</sub> H <sub>9</sub> N <sub>4</sub> O <sub>6</sub> <sup>-</sup>	-0.2	C <sub>3</sub> H <sub>6</sub> O <sub>3</sub>	dihydroxyacetone
45	293.126	C <sub>13</sub> H <sub>17</sub> N <sub>4</sub> O <sub>4</sub> <sup>-</sup>	0.2	C <sub>7</sub> H <sub>14</sub> O	heptanol
34	295.068	C <sub>11</sub> H <sub>11</sub> N <sub>4</sub> O <sub>6</sub> <sup>-</sup>	-0.7	C <sub>5</sub> H <sub>8</sub> O <sub>3</sub>	proposed in Scheme 2
39,44,46,50,51	329.211	C <sub>21</sub> H <sub>29</sub> O <sub>3</sub> <sup>-</sup>	-0.7	C <sub>21</sub> H <sub>30</sub> O <sub>3</sub>	proposed in Scheme 2
35,40,43	331.227	C <sub>21</sub> H <sub>31</sub> O <sub>3</sub> <sup>-</sup>	-0.2	C <sub>21</sub> H <sub>32</sub> O <sub>3</sub>	proposed in Scheme 2
33	339.131	C <sub>14</sub> H <sub>19</sub> N <sub>4</sub> O <sub>6</sub> <sup>-</sup>	0	C <sub>8</sub> H <sub>16</sub> O <sub>3</sub>	proposed in Scheme 2
36,38	345.207	C <sub>21</sub> H <sub>29</sub> O <sub>4</sub> <sup>-</sup>	-0.4	C <sub>21</sub> H <sub>30</sub> O <sub>4</sub>	proposed in Scheme 2
54	373.237	C <sub>23</sub> H <sub>33</sub> O <sub>4</sub> <sup>-</sup>	-0.6	C <sub>23</sub> H <sub>34</sub> O <sub>4</sub>	10-ethoxy-9-hydroxy-THC
55,56	399.203	C <sub>21</sub> H <sub>27</sub> N <sub>4</sub> O <sub>4</sub> <sup>-</sup>	-0.9	C <sub>15</sub> H <sub>24</sub> O	unidentified
49	399.290	C <sub>26</sub> H <sub>39</sub> O <sub>3</sub> <sup>-</sup>	-0.4	C <sub>26</sub> H <sub>40</sub> O <sub>3</sub>	unidentified
41	425.147	C <sub>21</sub> H <sub>21</sub> N <sub>4</sub> O <sub>6</sub> <sup>-</sup>	-0.1	C <sub>15</sub> H <sub>18</sub> O <sub>3</sub>	cannabispiran
37	303.196	C <sub>19</sub> H <sub>27</sub> O <sub>3</sub> <sup>-</sup>	-0.9	C <sub>19</sub> H <sub>28</sub> O <sub>3</sub>	cannabiglendol
	279.073	C <sub>11</sub> H <sub>11</sub> N <sub>4</sub> O <sub>5</sub> <sup>-</sup>	-0.3	C <sub>5</sub> H <sub>8</sub> O <sub>2</sub>	proposed in Scheme 2
	423.131	C <sub>21</sub> H <sub>19</sub> N <sub>4</sub> O <sub>6</sub> <sup>-</sup>	0	C <sub>15</sub> H <sub>16</sub> O <sub>3</sub>	cannabispirone-A
	321.120	C <sub>14</sub> H <sub>17</sub> N <sub>4</sub> O <sub>5</sub> <sup>-</sup>	-0.4	C <sub>8</sub> H <sub>14</sub> O <sub>2</sub>	proposed in Scheme 2
	305.125	C <sub>14</sub> H <sub>17</sub> N <sub>4</sub> O <sub>4</sub> <sup>-</sup>	-0.1	C <sub>8</sub> H <sub>14</sub> O	proposed in Scheme 2
	325.181	C <sub>21</sub> H <sub>25</sub> O <sub>3</sub> <sup>-</sup>	-0.1	C <sub>21</sub> H <sub>26</sub> O <sub>3</sub>	OH-cannabinol
	347.223	C <sub>21</sub> H <sub>31</sub> O <sub>4</sub> <sup>-</sup>	-0.2	C <sub>21</sub> H <sub>32</sub> O <sub>4</sub>	proposed in Scheme 2
	367.118	C <sub>21</sub> H <sub>19</sub> O <sub>6</sub> <sup>-</sup>	-0.8	C <sub>21</sub> H <sub>20</sub> O <sub>6</sub>	cannflavin B
	377.233	C <sub>22</sub> H <sub>33</sub> O <sub>5</sub> <sup>-</sup>	0.1	C <sub>21</sub> H <sub>32</sub> O <sub>3</sub> <sup>4a</sup>	proposed in Scheme 2
	393.228	C <sub>22</sub> H <sub>33</sub> O <sub>6</sub> <sup>-</sup>	-0.6	C <sub>21</sub> H <sub>32</sub> O <sub>4</sub> <sup>4a</sup>	proposed in Scheme 2
	401.146	C <sub>19</sub> H <sub>21</sub> N <sub>4</sub> O <sub>6</sub> <sup>-</sup>	-0.4	C <sub>13</sub> H <sub>18</sub> O <sub>3</sub>	proposed in Scheme 2
	415.162	C <sub>20</sub> H <sub>23</sub> N <sub>4</sub> O <sub>6</sub> <sup>-</sup>	-0.3	C <sub>14</sub> H <sub>20</sub> O <sub>3</sub>	unidentified
	507.224	C <sub>27</sub> H <sub>31</sub> N <sub>4</sub> O <sub>6</sub> <sup>-</sup>	0.2	C <sub>21</sub> H <sub>28</sub> O <sub>3</sub>	proposed in Scheme 2
Compound Identified from Vaping Aerosol of Pure VEA					
8	295.105	C <sub>12</sub> H <sub>15</sub> N <sub>4</sub> O <sub>5</sub> <sup>-</sup>	0	C <sub>6</sub> H <sub>12</sub> O <sub>2</sub>	proposed in Scheme 1
23	307.141	C <sub>14</sub> H <sub>19</sub> N <sub>4</sub> O <sub>4</sub> <sup>-</sup>	-0.9	C <sub>8</sub> H <sub>16</sub> O	proposed in Scheme 1
26	321.157	C <sub>15</sub> H <sub>21</sub> N <sub>4</sub> O <sub>4</sub> <sup>-</sup>	-0.7	C <sub>9</sub> H <sub>18</sub> O	proposed in Scheme 1
29	335.172	C <sub>16</sub> H <sub>23</sub> N <sub>4</sub> O <sub>4</sub> <sup>-</sup>	-0.2	C <sub>10</sub> H <sub>20</sub> O	proposed in Scheme 1
31	349.188	C <sub>17</sub> H <sub>25</sub> N <sub>4</sub> O <sub>4</sub> <sup>-</sup>	0.2	C <sub>11</sub> H <sub>22</sub> O	proposed in Scheme 1

Table 2. continued

peak labeled in chromatograph	calibrated $m/z$	corresponding ion	mass error (ppm)	molecular formula	proposed compound
24,28	377.219	$C_{19}H_{29}N_4O_4^-$	-0.9	$C_{13}H_{26}O$	proposed in Scheme 1
18	401.110	$C_{18}H_{17}N_4O_7^-$	-0.2	$C_{12}H_{14}O_4$	proposed in Scheme 1
22	483.189	$C_{24}H_{27}N_4O_7^-$	0.6	$C_{18}H_{24}O_4$	proposed in Scheme 1
25,27	511.220	$C_{26}H_{31}N_4O_7^-$	0.7	$C_{20}H_{28}O_4$	proposed in Scheme 1
30	525.236	$C_{27}H_{33}N_4O_7^-$	0.4	$C_{21}H_{30}O_4$	proposed in Scheme 1
	469.173	$C_{23}H_{25}N_4O_7^-$	-0.6	$C_{17}H_{22}O_4$	proposed in Scheme 1
	539.252	$C_{28}H_{35}N_4O_7^-$	0.7	$C_{22}H_{32}O_4$	proposed in Scheme 1
	553.267	$C_{29}H_{37}N_4O_7^-$	0.6	$C_{23}H_{34}O_4$	proposed in Scheme 1
	581.299	$C_{31}H_{41}N_4O_7^-$	1.3	$C_{25}H_{38}O_4$	proposed in Scheme 1

<sup>a</sup>The detected ion is the cluster ion of the molecule and  $HCOO^-$ .

Scheme 1. Proposed Thermal Degradation Pathway of VEA<sup>a</sup>

<sup>a</sup>The corresponding peaks in Table 2 are labeled. The degradation products  $C_{17}H_{22}O_4$ ,  $C_{22}H_{32}O_4$ ,  $C_{23}H_{34}O_4$ , and  $C_{25}H_{38}O_4$  are identified but not numbered due to the relatively small peak intensity.

known, it is likely that extensive hydrogen bonding can change the physical characteristics of the e-liquid that could lead to aerosolization differences.

Thermal degradation or oxidation products of VEA and THC were observed at the measured coil temperature of  $450 \pm 20^\circ F$  ( $232^\circ C$ ), similar to the temperature that VEA began to degrade in the work of Riordan-Short et al.<sup>27</sup> Single-ion chromatograms

(SIC) of aerosolized components from VEA, THC oil, and the 1:1 mixture (Figure 2) show that the aerosol composition is quite complex but that aerosols from the vaped 1:1 mixture of THC oil and VEA more closely resembles that from the vaped THC oil. Carbonyls and acids that can be generated from the thermal degradation of both VEA and THC oil (Figure 2, black line) are the small compounds such as formaldehyde,

**Table 3. Quantification of the Proposed Thermal Degradation Carbonyl and Organic Acid Compounds Generated by the Aerosolized e-Liquid of VEA, VEA/THC Oil, and THC Oil at a Temperature of  $450 \pm 20$  °F ( $232$  °C)<sup>a</sup>**

	THC ( $\mu\text{g}/\text{mg}$ )	THC/VEA ( $\mu\text{g}/\text{mg}$ )	VEA ( $\mu\text{g}/\text{mg}$ )
formaldehyde	0.01 $\pm$ 0.002	0.03 $\pm$ 0.004	0.73 $\pm$ 0.09
acetaldehyde	1.08 $\pm$ 0.10	0.83 $\pm$ 0.18	0.41 $\pm$ 0.05
formic acid	0.005 $\pm$ 0.001	0.03 $\pm$ 0.01	0.06 $\pm$ 0.02
acetic acid	0.008 $\pm$ 0.001	0.03 $\pm$ 0.004	0.10 $\pm$ 0.02
acetone	1.33 $\pm$ 0.31	1.63 $\pm$ 0.39	1.80 $\pm$ 0.49
butyraldehyde/ isobutyraldehyde	0.46 $\pm$ 0.08	0.65 $\pm$ 0.13	0.20 $\pm$ 0.10
valeraldehyde/ isovaleraldehyde	0.51 $\pm$ 0.11	0.66 $\pm$ 0.15	0.64 $\pm$ 0.30
hexanal/4- methylpentanal	0.05 $\pm$ 0.01	0.15 $\pm$ 0.03	2.29 $\pm$ 0.42
glyoxal	0.002 $\pm$ 0.001	0.005 $\pm$ 0.002	0.07 $\pm$ 0.02
methylglyoxal	0.04 $\pm$ 0.01	0.08 $\pm$ 0.03	0.08 $\pm$ 0.02
diacetyl/ $\text{C}_4\text{H}_6\text{O}_2$	0.02 $\pm$ 0.004	0.02 $\pm$ 0.01	0.07 $\pm$ 0.02
acrolein	0.005 $\pm$ 0.001	N.D.	0.02 $\pm$ 0.006
propionaldehyde	0.09 $\pm$ 0.02	0.08 $\pm$ 0.02	0.02 $\pm$ 0.004
glycoaldehyde	0.03 $\pm$ 0.01	0.13 $\pm$ 0.05	0.22 $\pm$ 0.07
methacrolein	0.06 $\pm$ 0.01	0.11 $\pm$ 0.02	0.20 $\pm$ 0.09
crotonaldehyde	0.007 $\pm$ 0.001	N.D.	N.D.
hydroxyacetone	0.38 $\pm$ 0.16	0.12 $\pm$ 0.05	0.12 $\pm$ 0.05
lactaldehyde	0.16 $\pm$ 0.07	0.04 $\pm$ 0.02	0.04 $\pm$ 0.02
dihydroxyacetone	0.06 $\pm$ 0.02	0.07 $\pm$ 0.02	N.D.
glyceraldehyde	0.002 $\pm$ 0.001	0.005 $\pm$ 0.002	N.D.
heptanol	0.49 $\pm$ 0.16	0.52 $\pm$ 0.18	N.D.
$\text{C}_3\text{H}_8\text{O}_3$	0.04 $\pm$ 0.02	0.08 $\pm$ 0.03	N.D.
$\text{C}_8\text{H}_{16}\text{O}_3$	0.05 $\pm$ 0.02	0.16 $\pm$ 0.05	N.D.
$\text{C}_8\text{H}_{14}\text{O}_2$	0.11 $\pm$ 0.04	0.15 $\pm$ 0.05	N.D.
$\text{C}_8\text{H}_{14}\text{O}$	0.36 $\pm$ 0.11	0.50 $\pm$ 0.16	N.D.
$\text{C}_6\text{H}_{12}\text{O}_2$	N.D.	0.03 $\pm$ 0.01	0.11 $\pm$ 0.04
$\text{C}_8\text{H}_{16}\text{O}$	N.D.	0.11 $\pm$ 0.04	1.36 $\pm$ 0.48
$\text{C}_9\text{H}_{18}\text{O}$	N.D.	0.08 $\pm$ 0.03	0.14 $\pm$ 0.05
$\text{C}_{10}\text{H}_{20}\text{O}$	N.D.	N.D.	0.10 $\pm$ 0.03
$\text{C}_{11}\text{H}_{22}\text{O}$	N.D.	0.02 $\pm$ 0.01	0.06 $\pm$ 0.02
$\text{C}_{12}\text{H}_{14}\text{O}_4$	N.D.	0.007 $\pm$ 0.002	1.81 $\pm$ 0.57
$\text{C}_{17}\text{H}_{22}\text{O}_4$	N.D.	0.04 $\pm$ 0.02	0.32 $\pm$ 0.12
$\text{C}_{18}\text{H}_{24}\text{O}_4$	N.D.	N.D.	0.34 $\pm$ 0.11
$\text{C}_{20}\text{H}_{28}\text{O}_4$	N.D.	0.12 $\pm$ 0.06	0.62 $\pm$ 0.20
$\text{C}_{21}\text{H}_{30}\text{O}_4$	N.D.	N.D.	0.03 $\pm$ 0.01

<sup>a</sup>N.D.= not detected above the quantification limit.

acetaldehyde, acetone, diacetyl, glyoxal, etc., and their associated carboxylic acids (Table 2). The blue line in Figure 2 represents the carbonyls and acids only from the thermal degradation of VEA, and the magenta line represents both carbonyls and cannabinoids from the vaping aerosol of THC oil. Some isomers have ambiguous identification, e.g.,  $\text{C}_6\text{H}_{12}\text{O}$  (#19 in Table 2) can be assignable to either hexanal or 4-methylpentanal. While hexanal can be formed from terpenes,<sup>57</sup> 4-methylpentanal is uniquely formed from the thermal degradation VEA according to the proposed thermal degradation pathway in Scheme 1. Since  $\text{C}_6\text{H}_{12}\text{O}$  is highly enhanced in the VEA aerosol (Figure 2a), we assign the majority of this emission to 4-methylpentanal.

Approximately 10 carbonyls and acids (e.g., formaldehyde, isovaleraldehyde, acetic acid) identified in Table 2 have also been reported by Riordan-Short et al.<sup>27</sup> However, carbonyls with VEA-specific structures (e.g.,  $\text{C}_{12}\text{H}_{14}\text{O}_4$  in Table 2) are newly identified here (Schemes 1 and S1). Riordan-Short et al.

also identified several esters and alkanes with GC-MS. The lack of standard spectra for VEA-derived compounds in GC-MS libraries may have prevented the identification of these peaks previously. Moreover, some carbonyls identified by Riordan-Short et al. were not found in this work (e.g., 3,6-heptanedione). The cause of discrepancy is unknown; however, it could be hypothesized that it may be partially due to the difference in vaporization method (using a heated coil in a third-generation vaping device in this study, while Riordan-Short used a surrogate vaping environment).

To determine the influence of VEA on the formation of carbonyls, it is informative to normalize the mass of carbonyls produced by the particle mass collected (Table 1) at the same temperature (Table 3). Figure 3 shows the normalized mass of nine selected thermal degradation carbonyls from vaping VEA, THC oil, and their mixture at 450 °F (235 °C). Some carbonyls such as formaldehyde, hexanal/4-methylpentanal, glyoxal, and  $\text{C}_4\text{H}_6\text{O}_2$  (diacetyl and other isomers) were produced in higher abundance from VEA compared to THC oil. While e-cigarette users who use nicotine products will self-titrate nicotine intake,<sup>58,59</sup> there is also evidence that people who use higher potency cannabis for recreational purpose can also titrate their THC dose.<sup>60</sup> For high-VEA-mixture fractions, users who self-titrate may be exposed to high levels of VEA-related products.

Within the  $\text{C}_4$ – $\text{C}_6$  carbonyls shown in Figure 3, butyraldehyde, valeraldehyde, and hexanal appear to originate from the thermal degradation of cannabinoids and terpenes, which is consistent with Tang et al.,<sup>57</sup> while isobutyraldehyde, isovaleraldehyde, and 4-methylpentanal are from the thermal degradation of VEA (Scheme 1). Although some products like formaldehyde can be produced from both VEA and THC oil, the production of formaldehyde from VEA appears more favorable since it involves a bond cleavage at a more substituted carbon (Scheme 1, path a), which forms a more stable alkyl radical intermediates than those from the unbranched aliphatic side chain of THC.<sup>61,62</sup> The same logic applies to the generation of 4-methylpentanal from VEA, which dominates the distribution of the isomer pair over hexanal. The formation of glyoxal likewise may be enhanced in VEA due to the higher stability of radical intermediates. Diacetyl ( $\text{C}_4\text{H}_6\text{O}_2$ ) is thought to be a byproduct of cannabis plants.<sup>61</sup> However, the SIC of  $\text{C}_4\text{H}_6\text{O}_2$  in the vaped THC oil demonstrated multiple isomers of  $\text{C}_4\text{H}_6\text{O}_2$  in that mixture besides diacetyl. From VEA, diacetyl may be generated from the thermal-induced scission of the C–O bond on the acetyl group, which will form acyl radicals that combine to form diacetyl<sup>63</sup> (Scheme 1, path m). The formation of a  $\text{C}_4\text{H}_6\text{O}_2$  isomer, 3-oxobutanol, can also be rationalized (Scheme 1, path e); however, there was only one  $\text{C}_4\text{H}_6\text{O}_2$  peak in the vaping aerosol of pure VEA and it has the retention time of diacetyl-DNPH (~10.9 min) in our analytical method. Thus, we believe that diacetyl is the main  $\text{C}_4\text{H}_6\text{O}_2$  from VEA, while multiple isomers are likely formed when VEA and THC are vaped together.

In some cases, the THC/VEA mixture produced more carbonyl emissions per mg particle mass than the pure compounds (e.g., butyraldehyde/isobutyraldehyde, valeraldehyde/isovaleraldehyde, methylglyoxal). Although this trend is less clear within error, it may suggest some synergetic effects between THC and VEA. Moreover, the THC oil tended to produce a higher amount of acetaldehyde than VEA. VEA degradation may form acetaldehyde (Scheme 1), but the unbranched side chain of certain cannabinoids, such as THC

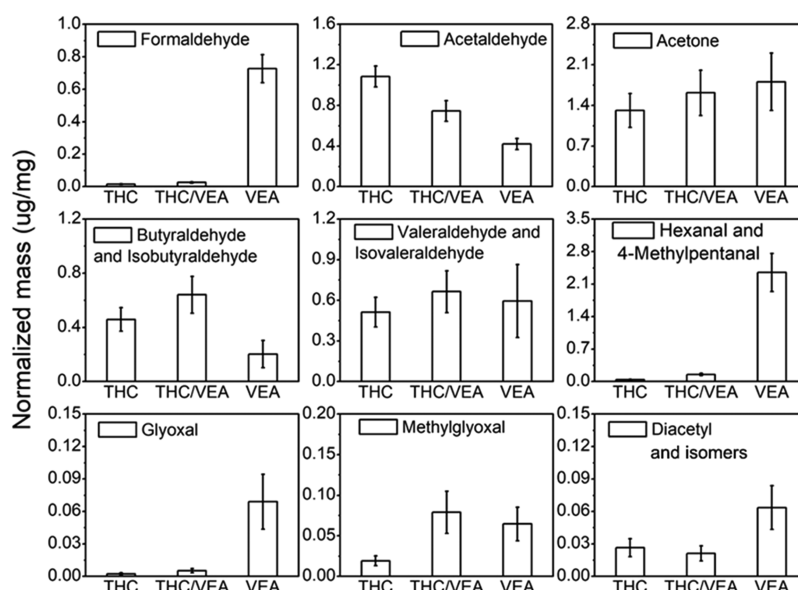


**Figure 3.** Mass of thermal degradation carbonyls normalized by particle mass-produced from vaping VEA, THC oil, and their 1:1 mixture at  $450 \pm 20$  °F ( $232$  °C).

and CBG (Scheme 2), provides more direct pathways for acetaldehyde formation.

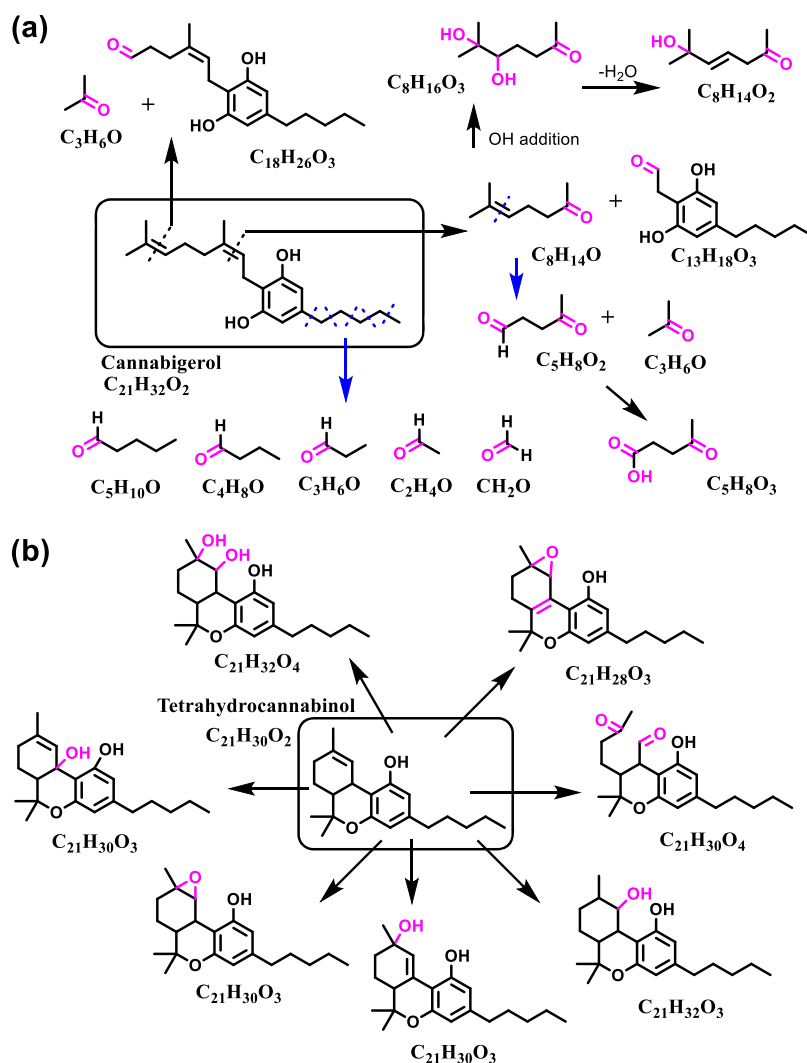
Scheme 2 shows that multiple cannabinoids identified in Table 2 may be formed as a result of reactive oxygen addition (in addition to bond cleavage). While analysis of the THC oil extract did not detect OH-functionalized cannabinoids in the original e-liquid (Figure S1), we cannot rule out the possibility that functionalized cannabinoids exist in the unvaped THC oil. Borille et al.<sup>48</sup> found 123 cannabinoid compounds or metabolites and eight noncannabinoid constituents in the extracts of cannabis plants by ESI-MS, with carbon number ranging from  $C_{15}$  to  $C_{55}$ . All molecular formulas of the THC oxidation products in Scheme 2b were also identified in cannabis extracts,<sup>64–69</sup> suggesting that oxidation from plant metabolism or during extraction could have occurred in addition to vaping.  $C_{19}H_{28}O_3$  is identified here as cannabiglendol- $C_3$ ;<sup>48,64</sup>  $C_{23}H_{34}O_4$  may have multiple isomers (e.g., cannabigerolic acid monomethyl ether or 10-ethoxy-9-hydroxytetrahydrocannabinol);<sup>48,70</sup> and  $C_{15}H_{16}O_3/C_{15}H_{18}O_3$  is identified as cannabispirenone/ cannabispiran.<sup>71,72</sup> Some compounds in Table 2 still remain unidentified (e.g.,  $C_{26}H_{40}O_3$ ).

Due to the uncertainty of the collection efficiency of cannabinoids through the silica cartridge, the quantification reported here for a number of cannabinoids (and oxidized cannabinoids) should be considered a lower limit (Table 4). Cannabinoid emissions per puff increase with temperature at the same e-liquid composition and decrease with VEA addition at the same temperature. Often, chemical emission trends follow the trends in particle mass emission (Table 1), but yield ratios ( $\mu\text{g}/\text{mg}$ ) will indicate if significant chemical transformations occurred during vaping. While the mass yields per mg of particle mass of CBG,  $\Delta^9$ -THC, CBC, cannabiglendol, OH-cannabinol, and cannflavin B increase with respect to temperature in the vaped THC oil aerosol, it decreases for all of the acids (THCA, CBDA, CBGA), cannabispirone-A, 10-ethoxy-9-hydroxy THC, and CBN. Compounds such as OH-cannabinol may increase with temperature because they are more efficiently vaporized or are formed through radical-initiated chemistry (Scheme S2), adding oxygen functional groups to the carbon skeleton of CBG

and THC (Scheme 2). The decreasing yield ratio of acids such as THCA is expected with temperature, as they may be degraded through decarboxylation more effectively at higher coil temperatures, a process that also occurs during the initial processing of THC oil, resulting in the formation of neutral cannabinoids (THC, CBD, CBG, respectively).<sup>73</sup> Thus, the large reservoir of THCA present prior to vaping (Figure S1) converts to THC while vaping in this third-generation mod device. The same process occurs from CGBA to CBG, which explains the increasing trend of CBG and THC with temperature. Thermal decarboxylation should be efficient with temperatures above  $350$  °F ( $177$  °C),<sup>74</sup> playing a role to increase the observed yield of neutral cannabinoids. The underlying reasons for the decreasing trend of CBN with temperature is not clear, as CBN is thought to be relatively thermally stable and may be produced from other cannabinoids.<sup>75</sup>

Interestingly, when VEA is added, the yields of cannabinoids per mg of particle mass increase at the same temperature (Figure 4) for most, but not all, observed compounds. Furthermore, the addition of VEA reverses the temperature trends for some cannabinoids such as THC and CBG, causing their net degradation with temperature. It appears, therefore, that the addition of VEA accelerated both the aerosolization and degradation of many cannabinoids. The reasons for these trends are not apparent, and we cannot rule out that the measurement of particle mass between the two systems introduces sufficient undocumented error to explain these trends. It is possible the cotton wick used for this study exhibited less efficient wicking for the more viscous VEA,<sup>76</sup> which may have caused higher localized temperatures for certain portions of the coil surface despite controlling the temperature in the center of the coil. The temperature, physical integrity of the coil, and the saturation of the wick were monitored to ensure excessive heating did not occur; however, the wicking material remains a limitation of this work as ceramic wicks are more generally used for viscous liquids. For cannabiglendol, OH-cannabinol, and Cannflavin B, a decrease in emission yield was observed when VEA was added. Each of these compounds has multiple polar OH groups that could hydrogen-bond with VEA,<sup>24</sup> which could prevent them



Scheme 2. Proposed Oxidation and Thermal Degradation Pathway of CBG and THC<sup>a</sup>.

<sup>a</sup>The corresponding peaks of carbonyls in Table 1 were labeled after the chemical formulas. The thermal degradation carbonyl products  $C_8H_{14}O$ ,  $C_8H_{14}O_2$ ,  $C_5H_8O_2$ , and  $C_{13}H_{18}O_3$  were identified but not labeled in Figure 2 due to the relatively small peak intensity.

from escaping the e-liquid, although it is not clear why this intermolecular interaction would be preferable to those that occur with other cannabinoids. These complex trends may warrant further study.

Multiple terpenoids were also quantified in the particles (Table 5). Notably, only  $C_{15}$  sesquiterpenes were observed, which are of sufficiently low volatility to remain in the particle and which could represent only a small fraction of the terpene diversity and quantity found in the THC oil extract from cannabis.<sup>77</sup> However, it was not possible to perform a quantification of terpenes in the original e-liquid to compare with that found in the particle composition due to issues pertaining to licensure. Many terpenoids, especially the nonfunctionalized  $C_{10}$  monoterpenes, are considered volatile organic compounds (VOCs); they would preferentially be emitted in the gas phase during vaping. Thus, these terpene observations represent a lower limit as the particle filtration and extraction steps may lose terpenes due to volatilization. The hydroxyl groups of cedrol and nerolidol also help reduce vapor pressure; it is not clear from these data if functionalized terpenes were generated through oxidation or were originally present in the e-liquid. While temperature increases the emissions of

terpenes per puff, temperature decreases the terpene yield per mg particle collected from the vaped THC oil (Figure 5). These data clearly suggest that terpenes are degraded with temperature in the vaping process. Unlike cannabinoids, the addition of VEA did not significantly change terpene yield per mg particle. An exception is cedrol, where the yield at medium temperature increased with VEA addition for unknown reasons.

The terpene yield data are consistent with other reports of terpene degradation. Meehan-Atrash et al.<sup>30</sup> identified degradation products from myrcene, limonene, and linalool, including methacrolein, hydroxyacetone, and methyl vinyl ketone.<sup>78</sup> Tang et al.<sup>57</sup> found 11 thermal degradation products from a mixture of terpenoids, 7 of them are carbonyls including formaldehyde, acetaldehyde, acetone, acrolein, methacrolein, valeraldehyde, and hexanal. The methacrolein formed from vaped THC oil (Table 3) likely originates from terpene degradation, and its enhancement with VEA addition may be due to the aforementioned acceleration of volatilization or chemistry, as well as its source from VEA.

**3.2. Chemical Mechanisms of Thermal Degradation and Oxidation of VEA and Cannabinoids.** VEA and cannabinoids are observed to chemically react in the e-cigarette

Table 4. Lower-Limit Concentrations of Select Cannabinoids in Vaping Aerosols from Vaped THC Oil and the Mixture of THC Oil and VEA (1:1, by Volume)<sup>a</sup>

	CBG ( $\mu\text{g/puff}$ )	$\Delta^2\text{-THC}$ ( $\mu\text{g/puff}$ )	CBC ( $\mu\text{g/puff}$ )	CBD A ( $\mu\text{g/puff}$ )	THCA ( $\mu\text{g/puff}$ )	CBN ( $\mu\text{g/puff}$ )	CBGA ( $\mu\text{g/puff}$ )	cannabispiron A ( $\mu\text{g/puff}$ )	10-OEt-9-OH- THC ( $\mu\text{g/puff}$ )	cannabispiran ( $\mu\text{g/puff}$ )	cannabiglendol ( $\mu\text{g/puff}$ )	OH- cannabinol ( $\mu\text{g/puff}$ )	cannflavin B ( $\mu\text{g/puff}$ )
THC oil (low T)	16 $\pm$ 4	76 $\pm$ 22	2.5 $\pm$ 0.8	0.3 $\pm$ 0.1	9 $\pm$ 1	35 $\pm$ 20	5 $\pm$ 1	58 $\pm$ 18	438 $\pm$ 68	92 $\pm$ 20	6 $\pm$ 3	1.2 $\pm$ 0.6	5 $\pm$ 2
THC oil (med T)	214 $\pm$ 106	1260 $\pm$ 853	58 $\pm$ 37	0.6 $\pm$ 0.1	19 $\pm$ 2	59 $\pm$ 16	11 $\pm$ 3	273 $\pm$ 105	620 $\pm$ 135	286 $\pm$ 73	95 $\pm$ 25	50 $\pm$ 17	115 $\pm$ 41
THC/VEA (low T)	1.6 $\pm$ 0.4	47 $\pm$ 14	1.1 $\pm$ 0.3	0.02 $\pm$ 0.01	1.5 $\pm$ 0.2	2.4 $\pm$ 1.4	0.5 $\pm$ 0.1	2.4 $\pm$ 0.7	15 $\pm$ 2	6 $\pm$ 1	N.D.	N.D.	N.D.
THC/VEA (med T)	111 $\pm$ 18	759 $\pm$ 110	37 $\pm$ 8	0.14 $\pm$ 0.04	6 $\pm$ 1	27 $\pm$ 18	6 $\pm$ 2	101 $\pm$ 16	221 $\pm$ 30	133 $\pm$ 13	1.3 $\pm$ 0.8	3 $\pm$ 1	13 $\pm$ 4
THC/VEA (high T)	206 $\pm$ 12	1575 $\pm$ 80	65 $\pm$ 4	0.3 $\pm$ 0.1	10 $\pm$ 1	34 $\pm$ 26	7 $\pm$ 1	149 $\pm$ 54	414 $\pm$ 47	184 $\pm$ 57	9 $\pm$ 7	11 $\pm$ 9	31 $\pm$ 26
	CBG ( $\mu\text{g/mg}$ )	$\Delta^2\text{-THC}$ ( $\mu\text{g/mg}$ )	CBC ( $\mu\text{g/mg}$ )	CBD A ( $\mu\text{g/mg}$ )	THCA ( $\mu\text{g/mg}$ )	CBN ( $\mu\text{g/mg}$ )	CBGA ( $\mu\text{g/mg}$ )	cannabispiron A ( $\mu\text{g/mg}$ )	10-OEt-9-OH- THC ( $\mu\text{g/mg}$ )	cannabispiran ( $\mu\text{g/mg}$ )	cannabiglendol ( $\mu\text{g/mg}$ )	OH-cannabinol ( $\mu\text{g/mg}$ )	cannflavin ( $\mu\text{g/mg}$ )
THC oil (low T)	13 $\pm$ 4	63 $\pm$ 21	2.1 $\pm$ 0.7	0.2 $\pm$ 0.1	7 $\pm$ 2	29 $\pm$ 18	4 $\pm$ 1	49 $\pm$ 17	365 $\pm$ 83	77 $\pm$ 21	5 $\pm$ 3	1.0 $\pm$ 0.5	4 $\pm$ 2
THC oil (med T)	20 $\pm$ 10	117 $\pm$ 81	5.3 $\pm$ 3.5	0.05 $\pm$ 0.01	2 $\pm$ 4	5 $\pm$ 2	1.0 $\pm$ 0.3	25 $\pm$ 11	57 $\pm$ 16	27 $\pm$ 8	9 $\pm$ 3	5 $\pm$ 2	11 $\pm$ 4
THC/VEA (low T)	74 $\pm$ 17	506 $\pm$ 111	25 $\pm$ 7	0.09 $\pm$ 0.03	4 $\pm$ 1	18 $\pm$ 13	4 $\pm$ 1	67 $\pm$ 16	147 $\pm$ 32	89 $\pm$ 17	0.9 $\pm$ 0.5	2 $\pm$ 1	8 $\pm$ 3
THC/VEA (high T)	41 $\pm$ 7	315 $\pm$ 55	13 $\pm$ 2	0.06 $\pm$ 0.02	2.0 $\pm$ 0.4	7 $\pm$ 5	2 $\pm$ 1	30 $\pm$ 12	83 $\pm$ 37	37 $\pm$ 37	1.7 $\pm$ 1.5	2.2 $\pm$ 1.8	6 $\pm$ 5

<sup>a</sup>Data are reported as mass of cannabinoid per puff ( $\mu\text{g/puff}$ ) and mass of cannabinoid per mg of particles ( $\mu\text{g/mg}$ ). Low-temperature range is 315  $\pm$  15  $^{\circ}\text{F}$  (157  $^{\circ}\text{C}$ ), medium-temperature range is 450  $\pm$  20  $^{\circ}\text{F}$  (232  $^{\circ}\text{C}$ ), and high-temperature range is 545  $\pm$  10  $^{\circ}\text{F}$  (285  $^{\circ}\text{C}$ ). N.D. = not detected.

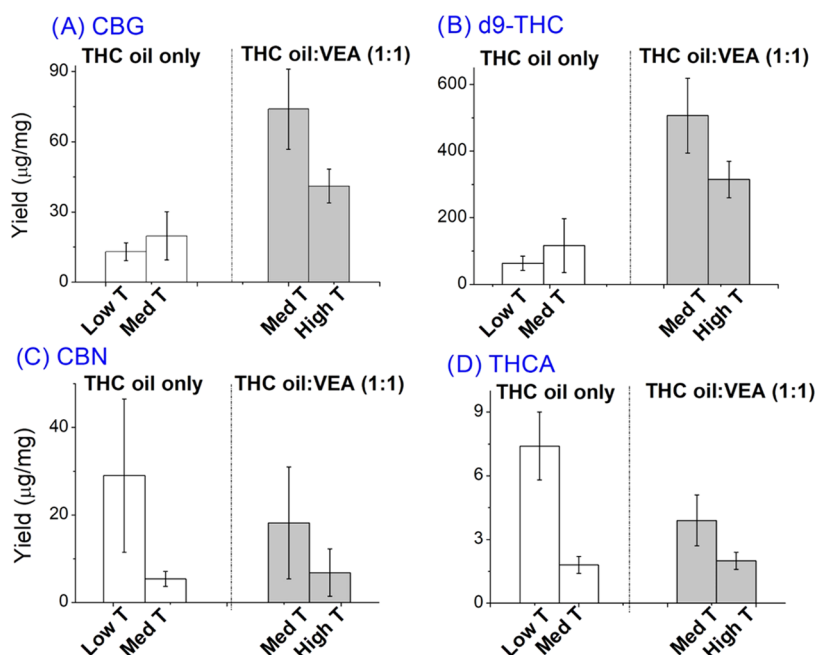


**Figure 4.** Mass of select cannabinoids normalized by particle mass-produced from vaping VEA, THC oil, and their 1:1 mixture at selected temperatures. Missing data occurred due to limited samples or undetectable particle mass. Low-temperature range is  $315 \pm 15$  °F ( $157$  °C), medium-temperature range is  $450 \pm 20$  °F ( $232$  °C), and high-temperature range is  $545 \pm 10$  °F ( $285$  °C).

**Table 5. Lower-Limit Concentrations of Select Cannabinoids in Vaping Aerosols from Vaped THC Oil and the Mixture of THC Oil and VEA (1:1, by Volume) at Two Temperature Ranges: Low  $315 \pm 15$  °F ( $157$  °C) and Medium  $450 \pm 20$  °F ( $232$  °C). N.D.= Not Detected.**

Sample	$\alpha$ -cedrene ( $\mu\text{g}/\text{puff}$ )	$\beta$ -caryophellene ( $\mu\text{g}/\text{puff}$ )	$\alpha$ -caryophellene ( $\mu\text{g}/\text{puff}$ )	E-nerolidol ( $\mu\text{g}/\text{puff}$ )	cedrol ( $\mu\text{g}/\text{puff}$ )
THC oil, low temp	$65.0 \pm 0.1$	$4.8 \pm 0.1$	$15.9 \pm 0.1$	$12.1 \pm 0.1$	$71.1 \pm 0.1$
THC oil, med. temp	$482.6 \pm 0.1$	$34.5 \pm 0.1$	$102.3 \pm 0.1$	$69.6 \pm 0.1$	$290.5 \pm 0.2$
THC/VEA, med. temp	$75.2 \pm 0.4$	$5.6 \pm 0.3$	$18.2 \pm 0.5$	$13.7 \pm 0.3$	$86.1 \pm 0.4$
	$\alpha$ -cedrene ( $\mu\text{g}/\text{mg}$ )	$\beta$ -caryophellene ( $\mu\text{g}/\text{mg}$ )	$\alpha$ -caryophellene ( $\mu\text{g}/\text{mg}$ )	E-nerolidol ( $\mu\text{g}/\text{mg}$ )	cedrol ( $\mu\text{g}/\text{mg}$ )
THC oil, low temp	$81 \pm 14$	$6 \pm 1$	$20 \pm 3$	$15 \pm 3$	$89 \pm 15$
THC oil, med. temp	$69 \pm 12$	$5 \pm 1$	$15 \pm 2$	$10 \pm 2$	$42 \pm 7$
THC/VEA, med. temp	$63 \pm 10$	$5 \pm 1$	$15 \pm 3$	$11 \pm 2$	$72 \pm 12$

vessel in a manner that is consistent with the degradation of PG and VG in conventional e-cigarettes, i.e., via the thermally induced degradation and/or ROS-induced degradation schemes described by Jensen et al.,<sup>79</sup> Li et al.,<sup>80,81</sup> and Diaz et al.,<sup>82</sup> among others. ROS such as OH radicals have been directly measured<sup>83–85</sup> and inferred by degradation product analyses,<sup>80</sup> in e-cigarette vessels and aerosol particles. However, OH sources in the vaping process are not well understood mechanistically. It had been suggested that OH can be formed from O<sub>2</sub> insertions into organic molecules, or from redox cycling of redox-active organics and/or transition metals.<sup>85,86</sup> Thermal degradation carbonyls and acids appear to be formed by C–C bond cleavage of the aliphatic side chain of VEA, with one carbonyl moiety formed at the site of each cleaved carbon (Scheme 1). This cleavage process produces two aldehydes at an unbranched site and aldehyde/ketone pair at a branched site. The degradation reactions may be initiated by bond homolysis, dehydration, or H-abstraction and addition by radicals such as OH, followed by the rapid reaction with O<sub>2</sub> to form peroxy radicals (RO<sub>2</sub>, Scheme S1).<sup>87,88</sup> The peroxy radicals can react with other RO<sub>2</sub> (or reducing agents) to form carbonyls or alkoxy (RO) radicals.<sup>89,90</sup> Alkoxy radicals may further react to form carbonyls (by  $\beta$ -scission), alcohols (by H-abstraction), and possibly alkenes (by

H<sub>2</sub>O elimination/radicals reaction).<sup>90–92</sup> The primary thermal degradation products may go through further oxidation steps and form more thermal degradation products (e.g., dicarbonyls such as glyoxal).<sup>90</sup> The RO<sub>2</sub>-based mechanisms have been well studied and shown to be important in various chemical systems, like the atmosphere, biological redox, or fuel combustion.<sup>93–96</sup> These mechanisms are consistent with observations, as the most abundant carbonyls observed in the VEA aerosol (Figure 2A, #18—C<sub>12</sub>H<sub>14</sub>O<sub>4</sub>, #23—C<sub>8</sub>H<sub>16</sub>O, #31—C<sub>11</sub>H<sub>22</sub>O) can be rationalized to be formed from the most stable radicals (benzylic and tertiary alkyl radical) in the first H-abstraction step (cleavage sites f, i, and l in Scheme 1). The benzylic radicals are stabilized by the conjugation effect from benzene ring and positive hyperconjugation from the adjacent C–H bonds.<sup>97–99</sup> The proposed thermal degradation pathway is also supported by the detection of alkenes (including 2,6-dimethyl-1-heptene and 1-pristene) by Riordan-Short et al.<sup>27</sup> and Mikheev et al.<sup>100</sup> since these compounds are predicted in the proposed mechanism. Thus, our observations suggest that the C–C single bonds on the side chain of VEA are easily oxidized and cleaved during the vaping process, which will cause the formation of a series of carbonyls that have VEA-specific structure and also alkenes and alcohols. These primary products may go through a further

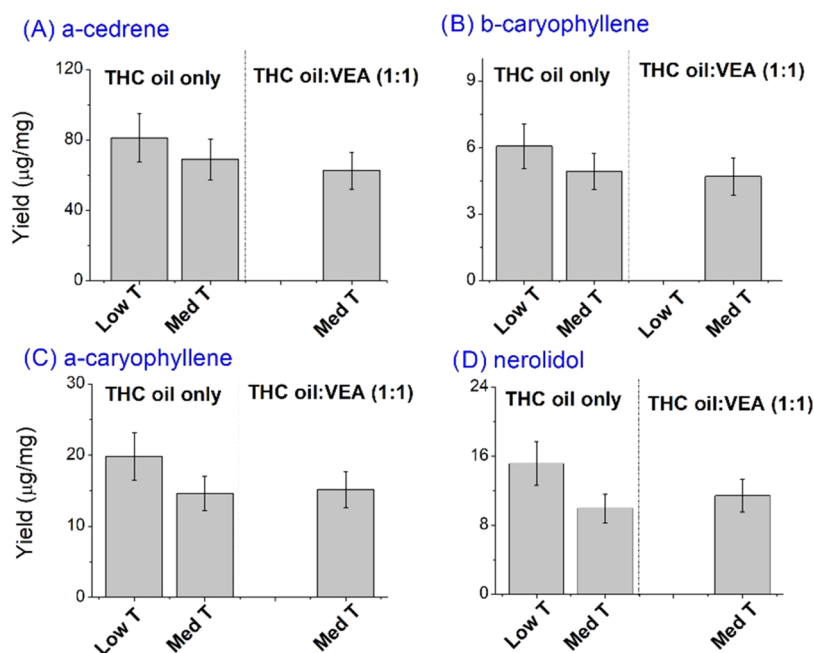


**Figure 5.** Mass of select terpenoids normalized by particle mass-produced from vaping VEA, THC oil, and their 1:1 mixture at selected temperatures. Missing data occurred due to limited samples or undetectable particle mass. Low-temperature range is  $315 \pm 15$  °F ( $157$  °C), medium-temperature range is  $450 \pm 20$  °F ( $232$  °C), and high-temperature range is  $545 \pm 10$  °F ( $285$  °C).

thermal degradation process to generate secondary thermal degradation products like acids and dicarbonyls.

OH radical can add to the unsaturated C=C bonds of  $\Delta^9$ THC and CBG to produce oxygen-functionalized products in the vaping aerosol of THC oil (Scheme 2). In contrast to VEA, the oxidation of CBG by OH proceeds primarily through the addition of the double bonds in the side chain, consistent with the oxidation of other alkenes.<sup>101–103</sup> The mechanism for the following steps is similar to the H-abstraction route. CBG may be the source of unique carbonyl products (e.g.,  $C_5H_8O_3$ ,  $C_8H_{14}O$ ) due to its second unsaturated side chain (Scheme 2a); the stepwise mechanism is shown in Scheme S2 for  $C_8H_{14}O$ . The oxidation may also occur on the unsaturated rings of cannabinoids, such as THC (Scheme 2b). However, unlike CBG, the allylic site of THC also enables substantial H-abstraction by OH (forming a resonance-stabilized radical) in addition to the OH addition occurring at the endocyclic C=C, preferentially forming the tertiary alkyl radical (Scheme S3). Multiple SIC peaks are found at the  $m/z$  representing oxidized products of cannabinoids, suggesting that different isomers abound. Our identification results are consistent with those of Carbone et al.,<sup>104</sup> who utilized NMR for identification. Carbone et al. indicated that peroxide products may also be formed during the oxidation process, a mechanism not shown in our schemes (as the ROOH is not well ionized in the electrospray ionization mass spectrometry used here) but would be consistent with  $RO_2$  chemistry.

#### 4. CONCLUSIONS

Although the third-generation temperature-programmable mod vaping device used in this work likely protects from excessive formation of toxic pyrolytic byproducts from cannabis extracts,<sup>74</sup> a myriad of thermal degradation and oxidation products were observed at the tested temperatures from cannabinoids, VEA, and terpenes under typical operating conditions. The addition of VEA had complex effects on

aerosolization efficiency and product formation that is supplemental to temperature. It is clear that the addition of VEA increases the formation of formaldehyde, glyoxal, 4-methylpentanal, methacrolein, and diacetyl, among other carbonyls per unit of particle mass. Self-titration of THC dose by users may enhance their inhalation exposure to VEA products when the VEA fraction in the e-liquid approaches 100%, due to increasingly higher production of certain carbonyls but increasingly lower emissions of THC and total particle mass. However, at the 1:1 mixture, the particle's THC yield is also enhanced compared to THC oil extract, which may negate increases in some carbonyl emissions for self-titration purposes. At the same time, VEA addition to the e-liquid had no effect on the observed yields of terpenoids, but a complex effect on the cannabinoid yield. Rich oxidative decomposition chemistry was observed for each compound class in the e-liquid. THC has a stronger tendency to degrade compared to VEA.<sup>105–107</sup> Regarding ketene that has been suggested to be formed by vaping or pyrolytic heating of VEA,<sup>28</sup> it is not clear whether it is identifiable with our methods or is not formed at the temperatures tested here. Products like duroquinone and durohydroquinone<sup>29,108–110</sup> are reported to be formed below a vaping coil temperature of  $300$  °C; however, we do not observe them with the preparation or detection methods used in this work. The selectivity and solubility of GC-MS extraction solvent could be a reason why products like quinones were not observed in the current study. These results underscore the fact that THC oil is a complex mixture, the complexity of which increases with thermal degradation chemistry and the addition of VEA. Further research on individual components is still needed for a better understanding of aerosol composition from vaping cannabis extracts and their mixtures with diluents.

## ■ ASSOCIATED CONTENT

### SI Supporting Information

The Supporting Information is available free of charge at <https://pubs.acs.org/doi/10.1021/acs.chemrestox.2c00064>.

Gas chromatography analysis of THC oil and proposed radical reaction mechanism for the thermal degradation of VEA, CBG, and THC (PDF)

## ■ AUTHOR INFORMATION

### Corresponding Author

Tran B. Nguyen – Department of Environmental Toxicology, University of California Davis, Davis, California 95616, United States; [orcid.org/0000-0001-9206-4359](https://orcid.org/0000-0001-9206-4359); Email: [tbn@ucdavis.edu](mailto:tbn@ucdavis.edu)

### Authors

Yichen Li – Department of Environmental Toxicology, University of California Davis, Davis, California 95616, United States; [orcid.org/0000-0001-6857-8106](https://orcid.org/0000-0001-6857-8106)

Jiayin Dai – Department of Environmental Toxicology, University of California Davis, Davis, California 95616, United States; [orcid.org/0000-0002-1786-5081](https://orcid.org/0000-0002-1786-5081)

Lillian N. Tran – Department of Environmental Toxicology, University of California Davis, Davis, California 95616, United States

Kent E. Pinkerton – Center for Health and the Environment, University of California Davis, Davis, California 95616, United States

Eliot R. Spindel – Oregon National Primate Research Center, Oregon Health & Science University, Beaverton, Oregon 97006, United States

Complete contact information is available at:

<https://pubs.acs.org/doi/10.1021/acs.chemrestox.2c00064>

### Author Contributions

T.B.N., K.E.P., E.R.S., and Y.L. designed the experiments. Y.L., L.N.T., and J.D. contributed original data and/or data analyses. K.E.P., E.R.S., and T.B.N. obtained the funding. T.B.N. and Y.L. prepared the draft manuscript. All co-authors reviewed and edited the manuscript.

### Notes

The authors declare no competing financial interest.

## ■ ACKNOWLEDGMENTS

The authors thank Dr. Brian Brandley and George Hodgins for supplying and testing the THC oil. This work was supported by the National Heart, Lung, and Blood Institute supplemental grant HL144384-02S1, NIH P51-OD011092, the UC Davis Cannabis and Hemp Research Center Research Investments in Cannabis and Hemp (RICH) grant, and the California Agricultural Experiment Station (grant no. CAD-ETX-2345-H) through the USDA National Institute of Food and Agriculture.

## ■ REFERENCES

- (1) Blagev, D. P.; Harris, D.; Dunn, A. C.; Guidry, D. W.; Grissom, C. K.; Lanspa, M. J. Clinical presentation, treatment, and short-term outcomes of lung injury associated with e-cigarettes or vaping: a prospective observational cohort study. *Lancet* **2019**, *394*, 2073–2083.
- (2) Chatham-Stephens, K.; Roguski, K.; Jang, Y.; Cho, P.; Jatlaoui, T. C.; Kabbani, S.; Glidden, E.; Ussery, E. N.; Trivers, K. F.; Evans, M. E.; et al. Characteristics of hospitalized and nonhospitalized patients in a

nationwide outbreak of e-cigarette, or vaping, product use–associated lung injury—United States, November 2019. *Morb. Mortal. Wkly. Rep.* **2019**, *68*, 1076.

- (3) Taylor, J.; Wiens, T.; Peterson, J.; Saravia, S.; Lunda, M.; Hanson, K.; Wogen, M.; D’Heilly, P.; Margetta, J.; Bye, M.; et al. Characteristics of e-cigarette, or vaping, products used by patients with associated lung injury and products seized by law enforcement—Minnesota, 2018 and 2019. *Morb. Mortal. Wkly. Rep.* **2019**, *68*, 1096.

- (4) Moritz, E. D.; Zapata, L. B.; Lekicavlili, A.; Glidden, E.; Annor, F. B.; Werner, A. K.; Ussery, E. N.; Hughes, M. M.; Kimball, A.; DeSisto, C. L.; et al. Update: characteristics of patients in a national outbreak of e-cigarette, or vaping, product use–associated lung injuries—United States, October 2019. *Morb. Mortal. Wkly. Rep.* **2019**, *68*, 985.

- (5) Kamal, M. A.; Raghunathan, V. Modulated phases of phospholipid bilayers induced by tocopherols. *Biochim. Biophys. Acta, Biomembr.* **2012**, *1818*, 2486–2493.

- (6) Fukuzawa, K.; Hayashi, K.; Suzuki, A. Effects of  $\alpha$ -tocopherol analogs on lysosome membranes and fatty acid monolayers. *Chem. Phys. Lipids* **1977**, *18*, 39–48.

- (7) Steiner, M. Vitamin E changes the membrane fluidity of human platelets. *Biochim. Biophys. Acta, Biomembr.* **1981**, *640*, 100–105.

- (8) Sagalowicz, L.; Guillot, S.; Acquistapace, S.; Schmitt, B.; Maurer, M.; Yagmur, A.; De Campo, L.; Rouvet, M.; Leser, M.; Glatter, O. Influence of vitamin E acetate and other lipids on the phase behavior of mesophases based on unsaturated monoglycerides. *Langmuir* **2013**, *29*, 8222–8232.

- (9) Navon, L.; Jones, C. M.; Ghinai, I.; King, B. A.; Briss, P. A.; Hacker, K. A.; Layden, J. E. Risk factors for e-cigarette, or vaping, product use–associated lung injury (EVALI) among adults who use e-cigarette, or vaping, products—Illinois, July–October 2019. *Morb. Mortal. Wkly. Rep.* **2019**, *68*, 1034.

- (10) Kalininskiy, A.; Bach, C. T.; Nacca, N. E.; Ginsberg, G.; Marraffa, J.; Navarette, K. A.; McGraw, M. D.; Croft, D. P. E-cigarette, or vaping, product use associated lung injury (EVALI): case series and diagnostic approach. *Lancet Respir. Med.* **2019**, *7*, 1017–1026.

- (11) Trivers, K. F.; Watson, C. V.; Neff, L. J.; Jones, C. M.; Hacker, K. Tetrahydrocannabinol (THC)-containing e-cigarette, or vaping, product use behaviors among adults after the onset of the 2019 outbreak of e-cigarette, or vaping, product use-associated lung injury (EVALI). *Addict. Behav.* **2021**, *121*, No. 106990.

- (12) MacMurdo, M.; Lin, C.; Saeedan, M. B.; Duxtader, E. E.; Mukhopadhyay, S.; Arrossi, V.; Reynolds, J.; Ghosh, S.; Choi, H. e-Cigarette or vaping product use-associated lung injury: clinical, radiologic, and pathologic findings of 15 cases. *Chest* **2020**, *157*, e181–e187.

- (13) Fedt, A.; Bhattarai, S.; Oelstrom, M. J. Vaping-Associated Lung Injury: A New Cause of Acute Respiratory Failure. *J. Adolesc. Health* **2020**, *66*, 754–757.

- (14) Thakrar, P. D.; Boyd, K. P.; Swanson, C. P.; Wideburg, E.; Kumbhar, S. S. E-cigarette, or vaping, product use-associated lung injury in adolescents: a review of imaging features. *Pediatr. Radiol.* **2020**, *50*, 338–344.

- (15) Lilly, C. M.; Khan, S.; Waksmundzki-Silva, K.; Irwin, R. S. Vaping-associated respiratory distress syndrome: case classification and clinical guidance. *Crit. Care Explor.* **2020**, *2*, No. e0081.

- (16) Blount, B. C.; Karwowski, M. P.; Shields, P. G.; Morel-Espinosa, M.; Valentin-Blasini, L.; Gardner, M.; Braselton, M.; Brosius, C. R.; Caron, K. T.; Chambers, D.; et al. Vitamin E acetate in bronchoalveolar-lavage fluid associated with EVALI. *N. Engl. J. Med.* **2020**, *382*, 697–705.

- (17) Krishnasamy, V. P.; Hollowell, B. D.; Ko, J. Y.; et al. Update: Characteristics of a Nationwide Outbreak of E-cigarette, or Vaping, Product Use–Associated Lung Injury—United States, August 2019–January 2020. *MMWR. Morb. Mortal. Wkly. Rep.* **2020**, *69*, No. 90.

- (18) Duffy, B.; Li, L.; Lu, S.; Durocher, L.; Dittmar, M.; Delaney-Baldwin, E.; Panawennage, D.; LeMaster, D.; Navarette, K.; Spink, D. Analysis of cannabinoid-containing fluids in illicit vaping cartridges recovered from pulmonary injury patients: identification of vitamin E acetate as a major diluent. *Toxics* **2020**, *8*, No. 8.

- (19) Eisenberg, Z.; Moy, D.; Lam, V.; Cheng, C.; Richard, J.; Burack, B. *Contaminant Analysis of Illicit vs Regulated Market Extracts*; Anresco Laboratories: San Francisco, 2019; p 26.
- (20) FDA, Lung Injuries Associated with Use of Vaping Products: <https://www.fda.gov/news-events/public-health-focus/lung-injuries-associated-use-vaping-products>, 2019.
- (21) Information for the Public, F. A., and Recommendations, Lung Injuries Associated with Use of Vaping Products. *U.S. Food & Drug Administration* 2020.
- (22) Food; Administration, D., Lung injuries associated with use of vaping products.
- (23) Espinosa, M. M.; Blount, B. C.; Valentin-Blasini, L. Liquid chromatography-tandem mass spectrometry method for measuring vitamin E acetate in bronchoalveolar lavage fluid. *J. Chromatogr. B* **2021**, *1171*, No. 122607.
- (24) Lanzarotta, A.; Falconer, T. M.; Flurer, R.; Wilson, R. A. Hydrogen bonding between tetrahydrocannabinol and vitamin E acetate in unvaped, aerosolized, and condensed aerosol e-liquids. *Anal. Chem.* **2020**, *92*, 2374–2378.
- (25) DiPasquale, M.; Gbadamosi, O.; Nguyen, M. H.; Castillo, S. R.; Rickerd, B. W.; Kelley, E. G.; Nagao, M.; Marquardt, D. A mechanical mechanism for vitamin E acetate in E-cigarette/Vaping-Associated lung injury. *Chem. Res. Toxicol.* **2020**, *33*, 2432–2440.
- (26) Matsumoto, S.; Fang, X.; Traber, M. G.; Jones, K. D.; Langelier, C.; Hayakawa Serpa, P.; Calfee, C. S.; Matthay, M. A.; Gotts, J. E. Dose-dependent pulmonary toxicity of aerosolized vitamin E acetate. *Am. J. Respir. Cell Mol. Biol.* **2020**, *63*, 748–757.
- (27) Seamus Riordan-Short, T. D. N.; Nahanni, S.; Noestheden, M.; O'Brien, R. *Thermal decomposition of vitamin E acetate in a surrogate vaping environment. Thermoscientific Customer Application Note*, 2020.
- (28) Wu, D.; O'Shea, D. F. Potential for release of pulmonary toxic ketene from vaping pyrolysis of vitamin E acetate. *Proc. Natl. Acad. Sci. U.S.A.* **2020**, *117*, 6349–6355.
- (29) Jiang, H.; Ahmed, C. S.; Martin, T. J.; Canchola, A.; Oswald, I. W.; Garcia, J. A.; Chen, J. Y.; Koby, K. A.; Buchanan, A. J.; Zhao, Z.; et al. Chemical and toxicological characterization of vaping emission products from commonly used vape juice diluents. *Chem. Res. Toxicol.* **2020**, *33*, 2157–2163.
- (30) Meehan-Atrash, J.; Luo, W.; Strongin, R. M. Toxicant formation in dabbing: the terpene story. *ACS Omega* **2017**, *2*, 6112–6117.
- (31) Ciolino, L. A.; Falconer, T. M.; Ranieri, T. L.; Brueggemeyer, J. L.; Taylor, A. M.; Mohrhaus, A. S. EVALI Vaping Liquids Part 2: Mass Spectrometric Identification of Diluents and Additives. *Front. Chem.* **2021**, *9*, No. 849.
- (32) Meehan-Atrash, J.; Luo, W.; McWhirter, K. J.; Strongin, R. M. Aerosol gas-phase components from cannabis e-cigarettes and Dabbing: mechanistic insight and quantitative risk analysis. *ACS Omega* **2019**, *4*, 16111–16120.
- (33) Henry, T. S.; Kanne, J. P.; Kligerman, S. J. Imaging of Vaping-Associated Lung Disease. *N. Engl. J. Med.* **2019**, *381*, 1486–1487.
- (34) Butt, Y. M.; Smith, M. L.; Tazelaar, H. D.; Vaszar, L. T.; Swanson, K. L.; Cecchini, M. J.; Boland, J. M.; Bois, M. C.; Boyum, J. H.; Froemming, A. T.; Khoor, A.; Mira-Avendano, I.; Patel, A.; Larsen, B. T. Pathology of Vaping-Associated Lung Injury. *N. Engl. J. Med.* **2019**, *381*, 1780–1781.
- (35) Muthumalage, T.; Lucas, J. H.; Wang, Q.; Lamb, T.; McGraw, M. D.; Rahman, I. Pulmonary Toxicity and Inflammatory Response of Vape Cartridges Containing Medium-Chain Triglycerides Oil and Vitamin E Acetate: Implications in the Pathogenesis of EVALI. *Toxics* **2020**, *8*, 46.
- (36) Wagner, J.; Chen, W.; Vrdoljak, G. Vaping cartridge heating element compositions and evidence of high temperatures. *PLoS One* **2020**, *15*, No. e0240613.
- (37) Lynch, J.; Lorenz, L.; Brueggemeyer, J. L.; Lanzarotta, A.; Falconer, T. M.; Wilson, R. A. Simultaneous Temperature Measurements and Aerosol Collection During Vaping for the Analysis of  $\Delta$ -9-Tetrahydrocannabinol and Vitamin E Acetate Mixtures in Ceramic Coil Style Cartridges. *Front. Chem.* **2021**, *9*, No. 643.
- (38) Varlet, V.; Concha-Lozano, N.; Berthet, A.; Plateel, G.; Favrat, B.; De Cesare, M.; Lauer, E.; Augsburger, M.; Thomas, A.; Giroud, C. Drug vaping applied to cannabis: Is “Cannavaping” a therapeutic alternative to marijuana? *Sci. Rep.* **2016**, *6*, 25599.
- (39) Farsalinos, K. E.; Voudris, V.; Poulas, K. E-cigarettes generate high levels of aldehydes only in ‘dry puff’ conditions. *Addiction* **2015**, *110*, 1352–1356.
- (40) Stevens, R. *CORESTA Electronic Cigarette Task Force*, 2014.
- (41) Dibaji, S. A. R.; Guha, S.; Arab, A.; Murray, B. T.; Myers, M. R. Accuracy of commercial electronic nicotine delivery systems (ENDS) temperature control technology. *PLoS One* **2018**, *13*, No. e0206937.
- (42) Chen, W.; Wang, P.; Ito, K.; Fowles, J.; Shusterman, D.; Jaques, P. A.; Kumagai, K. Measurement of heating coil temperature for e-cigarettes with a “top-coil” clearomizer. *PLoS One* **2018**, *13*, No. e0195925.
- (43) LeBouf, R. F.; Ranpara, A.; Ham, J.; Aldridge, M.; Fernandez, E.; Williams, K.; Burns, D. A.; Stefaniak, A. B. Chemical Emissions From Heated Vitamin E Acetate—Insights to Respiratory Risks From Electronic Cigarette Liquid Oil Diluents Used in the Aerosolization of  $\Delta$ -9-THC-Containing Products. *Front. Public Health* **2022**, *9*, No. 765168.
- (44) Li, Y.; Burns, A. E.; Burke, G. J.; Poindexter, M. E.; Madl, A. K.; Pinkerton, K. E.; Nguyen, T. B. Application of High-Resolution Mass Spectrometry and a Theoretical Model to the Quantification of Multifunctional Carbonyls and Organic Acids in e-Cigarette Aerosol. *Environ. Sci. Technol.* **2020**, *54*, 5640–5650.
- (45) Dibaji, S. A. R.; Guha, S.; Arab, A.; Murray, B. T.; Myers, M. R. Accuracy of commercial electronic nicotine delivery systems (ENDS) temperature control technology. *PLoS One* **2018**, *13*, No. e0206937.
- (46) Coresta, E.; Force, C. T. Routine analytical machine for e-cigarette aerosol generation and collection—definitions and standard conditions *Paris, CORESTA*, 2015.
- (47) Li, Y.; Burns, A. E.; Tran, L. N.; Abellar, K. A.; Poindexter, M.; Li, X.; Madl, A. K.; Pinkerton, K. E.; Nguyen, T. B. Impact of e-Liquid Composition, Coil Temperature, and Puff Topography on the Aerosol Chemistry of Electronic Cigarettes. *Chem. Res. Toxicol.* **2021**, *34*, 1640–1654.
- (48) Borille, B. T.; Ortiz, R. S.; Mariotti, K. C.; Vanini, G.; Tose, L. V.; Filgueiras, P. R.; Marcelo, M. C.; Ferrão, M. F.; Anzanello, M. J.; Limberger, R. P.; Romão, W. Chemical profiling and classification of cannabis through electrospray ionization coupled to Fourier transform ion cyclotron resonance mass spectrometry and chemometrics. *Anal. Methods* **2017**, *9*, 4070–4081.
- (49) Hollis, J.; Harper, T.; Macherone, A. *Terpenes Analysis in Cannabis Products by Liquid Injection using the Agilent Intuvo 9000/5977B GC/MS System*, 2020.
- (50) Sigma Aldrich, Complete Workflow for Comprehensive Cannabis Terpenes Analysis. <https://www.sigmaaldrich.com/US/en/technical-documents/protocol/analytical-chemistry/small-molecule-hplc/cannabis-testing>.
- (51) Sleiman, M.; Logue, J. M.; Montesinos, V. N.; Russell, M. L.; Litter, M. I.; Gundel, L. A.; Destailats, H. Emissions from electronic cigarettes: key parameters affecting the release of harmful chemicals. *Environ. Sci. Technol.* **2016**, *50*, 9644–9651.
- (52) Uchiyama, S.; Noguchi, M.; Sato, A.; Ishitsuka, M.; Inaba, Y.; Kunugita, N. Determination of Thermal Decomposition Products Generated from E-Cigarettes. *Chem. Res. Toxicol.* **2020**, *33*, 576–583.
- (53) EFSA Panel on Food Contact Materials; Flavourings, E.; Aids, P. Safety assessment of the substance  $\alpha$ -tocopherol acetate for use in food contact materials. *EFSA J.* **2016**, *14*, 4412.
- (54) Munjal, M.; Stodghill, S. P.; ElSohly, M. A.; Repka, M. A. Polymeric systems for amorphous  $\Delta$ -9-tetrahydrocannabinol produced by a hot-melt method. Part I: Chemical and thermal stability during processing. *J. Pharm. Sci.* **2006**, *95*, 1841–1853.
- (55) Karrer, P.; Stähelin, M. Über zwei neue Homologe des  $\alpha$ -Tocopherols. *Helv. Chim. Acta* **1945**, *28*, 438–443.
- (56) Fan, C.; Liu, Y.; Sebbah, T.; Cao, X. A Theoretical Study on Terpene-Based Natural Deep Eutectic Solvent: Relationship between

Viscosity and Hydrogen-Bonding Interactions. *Global Challenges* **2021**, 5, No. 2000103.

(57) Tang, X.; Cancelada, L.; Rapp, V. H.; Russell, M. L.; Maddalena, R. L.; Litter, M. I.; Gundel, L. A.; Destailats, H. Emissions from Heated Terpenoids Present in Vaporizable Cannabis Concentrates. *Environ. Sci. Technol.* **2021**, 55, 6160–6170.

(58) Dawkins, L. E.; Kimber, C. F.; Doig, M.; Feyerabend, C.; Corcoran, O. Self-titration by experienced e-cigarette users: blood nicotine delivery and subjective effects. *Psychopharmacology* **2016**, 233, 2933–2941.

(59) Smets, J.; Baeyens, F.; Chaumont, M.; Adriaens, K.; Van Gucht, D. When less is more: vaping low-nicotine vs. high-nicotine e-liquid is compensated by increased wattage and higher liquid consumption. *Int. J. Environ. Res. Public Health* **2019**, 16, No. 723.

(60) Leung, J.; Stjepanović, D.; Dawson, D.; Hall, W. D. Do Cannabis Users Reduce Their THC Dosages When Using More Potent Cannabis Products? A Review. *Front. Psychiatry* **2021**, 12, No. 163.

(61) Kossiakoff, A.; Rice, F. O. Thermal decomposition of hydrocarbons, resonance stabilization and isomerization of free radicals. *J. Am. Chem. Soc.* **1943**, 65, 590–595.

(62) Hioe, J.; Zipse, H. Radical stability and its role in synthesis and catalysis. *Org. Biomol. Chem.* **2010**, 8, 3609–3617.

(63) Rivaton, A.; Mailhot, B.; Soulestin, J.; Varghese, H.; Gardette, J. L. Comparison of the photochemical and thermal degradation of bisphenol-A polycarbonate and trimethylcyclohexane–polycarbonate. *Polym. Degrad. Stab.* **2002**, 75, 17–33.

(64) ElSohly, M. A.; Slade, D. Chemical constituents of marijuana: the complex mixture of natural cannabinoids. *Life Sci.* **2005**, 78, 539–548.

(65) Fishedick, J. T.; Hazekamp, A.; Erkelens, T.; Choi, Y. H.; Verpoorte, R. Metabolic fingerprinting of Cannabis sativa L., cannabinoids and terpenoids for chemotaxonomic and drug standardization purposes. *Phytochemistry* **2010**, 71, 2058–2073.

(66) Tettey, J. N.; Crean, C.; Rodrigues, J.; Yap, T. W. A.; Lim, J. L. W.; Lee, H. Z. S.; Ching, M. United Nations Office on Drugs and Crime: recommended methods for the identification and analysis of synthetic cannabinoid receptor agonists in seized materials. *Forensic Sci. Int. Synerg.* **2021**, 3, No. 100129.

(67) Radwan, M. M.; Ross, S. A.; Slade, D.; Ahmed, S. A.; Zulfqar, F.; ElSohly, M. A. Isolation and characterization of new cannabis constituents from a high potency variety. *Planta Med.* **2008**, 74, 267.

(68) Radwan, M. M.; ElSohly, M. A.; El-Alfy, A. T.; Ahmed, S. A.; Slade, D.; Husni, A. S.; Manly, S. P.; Wilson, L.; Seale, S.; Cutler, S. J.; Ross, S. A. Isolation and pharmacological evaluation of minor cannabinoids from high-potency Cannabis sativa. *J. Nat. Prod.* **2015**, 78, 1271–1276.

(69) Radwan, M. M.; ElSohly, M. A.; Slade, D.; Ahmed, S. A.; Khan, I. A.; Ross, S. A. Biologically active cannabinoids from high-potency Cannabis sativa. *J. Nat. Prod.* **2009**, 72, 906–911.

(70) Eiras, M. M.; De Oliveira, D.; Ferreira, M.; Benassi, M.; Cazenave, S.; Catharino, R. Fast fingerprinting of cannabinoid markers by laser desorption ionization using silica plate extraction. *Anal. Methods* **2014**, 6, 1350–1352.

(71) Vázquez-Ocín, P.; Marti, G.; Bonhomme, M.; Mathis, F.; Fournier, S.; Bertani, S.; Maciuk, A., Cannabinoids vs. whole metabolome: relevance of cannabinomics in analyzing Cannabis varieties. *bioRxiv* 2021.

(72) Pavlovic, R.; Panseri, S.; Giupponi, L.; Leoni, V.; Citti, C.; Cattaneo, C.; Cavaletto, M.; Giorgi, A. Phytochemical and ecological analysis of two varieties of hemp (Cannabis sativa L.) grown in a mountain environment of Italian Alps. *Front. Plant Sci.* **2019**, 10, No. 1265.

(73) Veress, T.; Szanto, J.; Leisztner, L. Determination of cannabinoid acids by high-performance liquid chromatography of their neutral derivatives formed by thermal decarboxylation: I. Study of the decarboxylation process in open reactors. *J. Chromatogr. A* **1990**, 520, 339–347.

(74) Giroud, C.; De Cesare, M.; Berthet, A.; Varlet, V.; Concha-Lozano, N.; Favrat, B. E-Cigarettes: A Review of New Trends in Cannabis Use. *Int. J. Environ. Res. Public Health* **2015**, 12, 9988–10008.

(75) Meija, J.; McRae, G.; Miles, C. O.; Melanson, J. E. Thermal stability of cannabinoids in dried cannabis: a kinetic study. *Anal. Bioanal. Chem.* **2022**, 414, 377–384.

(76) Strongin, R. M. E-cigarette chemistry and analytical detection. *Annu. Rev. Anal. Chem.* **2019**, 12, 23–39.

(77) Hanuš, L. O.; Hod, Y. Terpenes/Terpenoids in Cannabis: Are They Important? *Med. Cannabis Cannabinoids* **2020**, 3, 25–60.

(78) Meehan-Atrash, J.; Luo, W.; McWhirter, K. J.; Dennis, D. G.; Sarlah, D.; Jensen, R. P.; Afreh, I.; Jiang, J.; Barsanti, K. C.; Ortiz, A.; Strongin, R. M. The influence of terpenes on the release of volatile organic compounds and active ingredients to cannabis vaping aerosols. *RSC Adv.* **2021**, 11, 11714–11723.

(79) Jensen, R. P.; Strongin, R. M.; Peyton, D. H. Solvent chemistry in the electronic cigarette reaction vessel. *Sci. Rep.* **2017**, 7, No. 42549.

(80) Li, Y.; Burns, A. E.; Tran, L. N.; Abellar, K. A.; Poindexter, M.; Li, X.; Madl, A. K.; Pinkerton, K. E.; Nguyen, T. B. Impact of e-Liquid Composition, Coil Temperature, and Puff Topography on the Aerosol Chemistry of Electronic Cigarettes. *Chem. Res. Toxicol.* **2021**, 34, 1640–1654.

(81) Li, Y.; Burns, A. E.; Burke, G. J. P.; Poindexter, M. E.; Madl, A. K.; Pinkerton, K. E.; Nguyen, T. B. Application of High-Resolution Mass Spectrometry and a Theoretical Model to the Quantification of Multifunctional Carbonyls and Organic Acids in e-Cigarette Aerosol. *Environ. Sci. Technol.* **2020**, 54, 5640–5650.

(82) Diaz, E.; Sad, M. E.; Iglesias, E. Homogeneous oxidation reactions of propanediols at low temperatures. *ChemSusChem* **2010**, 3, 1063–1070.

(83) Bitzer, Z. T.; Goel, R.; Reilly, S. M.; Bhangu, G.; Trushin, N.; Foulds, J.; Muscat, J.; Richie, J. P. Emissions of Free Radicals, Carbonyls, and Nicotine from the NIDA Standardized Research Electronic Cigarette and Comparison to Similar Commercial Devices. *Chem. Res. Toxicol.* **2019**, 32, 130–138.

(84) Bitzer, Z. T.; Goel, R.; Reilly, S. M.; Elias, R. J.; Silakov, A.; Foulds, J.; Muscat, J.; Richie, J. P. Effect of flavoring chemicals on free radical formation in electronic cigarette aerosols. *Free Radicals Biol. Med.* **2018**, 120, 72–79.

(85) Son, Y.; Mishin, V.; Laskin, J. D.; Mainelis, G.; Wackowski, O. A.; Delnevo, C.; Schwander, S.; Khlystov, A.; Samburova, V.; Meng, Q. Hydroxyl Radicals in E-Cigarette Vapor and E-Vapor Oxidative Potentials under Different Vaping Patterns. *Chem. Res. Toxicol.* **2019**, 32, 1087–1095.

(86) Laino, T.; Tuma, C.; Moor, P.; Martin, E.; Stolz, S.; Curioni, A. Mechanisms of propylene glycol and triacetin pyrolysis. *J. Phys. Chem. A* **2012**, 116, 4602–4609.

(87) Davidson, D. F.; Herbon, J.; Horning, D.; Hanson, R. OH concentration time histories in n-alkane oxidation. *Int. J. Chem. Kinet.* **2001**, 33, 775–783.

(88) Houle, F. A.; Hinsberg, W.; Wilson, K. Oxidation of a model alkane aerosol by OH radical: the emergent nature of reactive uptake. *Phys. Chem. Chem. Phys.* **2015**, 17, 4412–4423.

(89) Bennett, J. E.; Summers, R. Product studies of the mutual termination reactions of sec-alkylperoxy radicals: Evidence for non-cyclic termination. *Can. J. Chem.* **1974**, 52, 1377–1379.

(90) Ruehl, C. R.; Nah, T.; Isaacman, G.; Worton, D. R.; Chan, A. W.; Kolesar, K. R.; Cappa, C. D.; Goldstein, A. H.; Wilson, K. R. The influence of molecular structure and aerosol phase on the heterogeneous oxidation of normal and branched alkanes by OH. *J. Phys. Chem. A* **2013**, 117, 3990–4000.

(91) Atkinson, R. Atmospheric reactions of alkoxy and  $\beta$ -hydroxyalkoxy radicals. *Int. J. Chem. Kinet.* **1997**, 29, 99–111.

(92) Baldwin, R.; Walker, R. *Elementary Reactions in the Oxidation of Alkenes*, Symposium (International) on Combustion, Elsevier, 1981; pp 819–829.

(93) Wang, Z.; Ehn, M.; Rissanen, M. P.; Garmash, O.; Quéléver, L.; Xing, L.; Monge-Palacios, M.; Rantala, P.; Donahue, N. M.; Berndt, T.; Sarathy, S. M. Efficient alkane oxidation under combustion engine and atmospheric conditions. *Commun. Chem.* **2021**, 4, 1–8.

(94) Calvert, J. G.; Derwent, R. G.; Orlando, J. J.; Wallington, T. J.; Tyndall, G. S. *Mechanisms of Atmospheric Oxidation of the Alkanes*; Oxford University Press, 2008.

(95) Carter, W. P.; Darnall, K. R.; Lloyd, A. C.; Winer, A. M.; Pitts, J. N., Jr. Evidence for alkoxy radical isomerization in photooxidations of C4–C6 alkanes under simulated atmospheric conditions. *Chem. Phys. Lett.* **1976**, *42*, 22–27.

(96) George, I. J.; Abbatt, J. Heterogeneous oxidation of atmospheric aerosol particles by gas-phase radicals. *Nat. Chem.* **2010**, *2*, 713.

(97) Chatgililoglu, C.; Ingold, K.; Scaiano, J. Rate constants and Arrhenius parameters for the reactions of primary, secondary, and tertiary alkyl radicals with tri-*n*-butyltin hydride. *J. Am. Chem. Soc.* **1981**, *103*, 7739–7742.

(98) Zipse, H. Radical stability—a theoretical perspective. In *Radicals in Synthesis I*; Springer, 2006; pp 163–189.

(99) Gryn'ova, G.; Marshall, D. L.; Blanksby, S. J.; Coote, M. L. Switching radical stability by pH-induced orbital conversion. *Nat. Chem.* **2013**, *5*, 474–481.

(100) Mikheev, V. B.; Klupinski, T. P.; Ivanov, A.; Lucas, E. A.; Strozler, E. D.; Fix, C. Particle size distribution and chemical composition of aerosolized vitamin E acetate. *Aerosol Sci. Technol.* **2020**, *54*, 993–998.

(101) Teng, A. P.; Crounse, J.; Lee, L.; St Clair, J.; Cohen, R.; Wennberg, P. Hydroxy nitrate production in the OH-initiated oxidation of alkenes. *Atmos. Chem. Phys.* **2015**, *15*, 4297–4316.

(102) Sprengnether, M.; Demerjian, K. L.; Donahue, N. M.; Anderson, J. G. Product analysis of the OH oxidation of isoprene and 1,3-butadiene in the presence of NO. *J. Geophys. Res.: Atmos.* **2002**, *107*, ACH 8-1–ACH 8-13.

(103) La, Y. S.; Camredon, M.; Ziemann, P.; Valorso, R.; Matsunaga, A.; Lannuque, V.; Lee-Taylor, J.; Hodzic, A.; Madronich, S.; Aumont, B. Impact of chamber wall loss of gaseous organic compounds on secondary organic aerosol formation: explicit modeling of SOA formation from alkane and alkene oxidation. *Atmos. Chem. Phys.* **2016**, *16*, 1417–1431.

(104) Carbone, M.; Castelluccio, F.; Daniele, A.; Sutton, A.; Ligresti, A.; Di Marzo, V.; Gavagnin, M. Chemical characterisation of oxidative degradation products of  $\Delta^9$ -THC. *Tetrahedron* **2010**, *66*, 9497–9501.

(105) Gaoni, Y.; Mechoulam, R. Isolation, structure, and partial synthesis of an active constituent of hashish. *J. Am. Chem. Soc.* **1964**, *86*, 1646–1647.

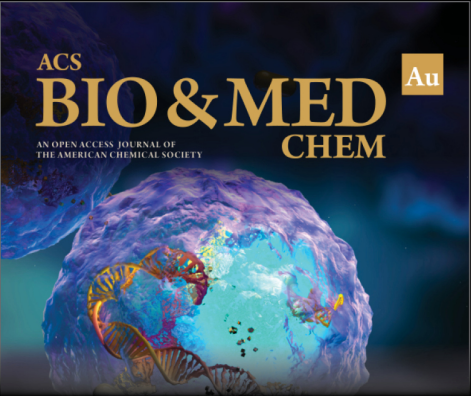
(106) Adams, R.; Cain, C.; McPhee, W.; Wearn, R. Structure of Cannabidiol. XII. Isomerization to Tetrahydrocannabinols. *J. Am. Chem. Soc.* **1941**, *63*, 2209–2213.

(107) Bolognesi, C.; Castle, L.; Cravedi, J.-P.; Engel, K.-H.; Fowler, P.; Franz, R.; Grob, K.; Gurtler, R.; Husoy, T.; Karenlampi, S. Safety assessment of the substance diethyl [[3, 5-bis (1, 1-dimethylethyl)-4-hydroxyphenyl] methyl] phosphonate, for use in food contact materials. *EFSA J.* **2016**, *14*, No. e04536.

(108) Tang, C.; Tao, G.; Wang, Y.; Liu, Y.; Li, J. Identification of  $\alpha$ -Tocopherol and Its Oxidation Products by Ultra-Performance Liquid Chromatography Coupled with Quadrupole Time-of-Flight Mass Spectrometry. *J. Agric. Food Chem.* **2020**, *68*, 669–677.

(109) Kovach, A. L.; Carter, R. R.; Thornburg, J. W.; Wiethe, R.; Fennell, T. R.; Wiley, J. L. Thermal Degradants Identified from the Vaping of Vitamin E Acetate. *J. Anal. Toxicol.* **2021**, No. bkab109.


(110) Canchola, A.; Ahmed, C. S.; Chen, K.; Chen, J. Y.; Lin, Y.-H. Formation of Redox-Active Duroquinone from Vaping of Vitamin E Acetate Contributes to Oxidative Lung Injury. *Chem. Res. Toxicol.* **2022**, *35*, 254–264.




ACS  
**BIO & MED**  
AN OPEN ACCESS JOURNAL OF  
THE AMERICAN CHEMICAL SOCIETY  
**CHEM**  
Au

Editor-in-Chief: **Prof. Shelley D. Minteer**, University of Utah, USA

Deputy Editor  
**Prof. Squire J. Booker**  
Pennsylvania State University, USA

**Open for Submissions** 

pubs.acs.org/biomedchemau  ACS Publications  
Most Trusted. Most Cited. Most Read.